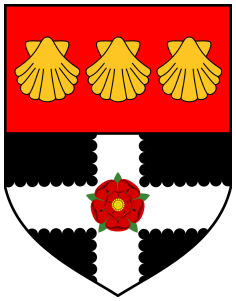

UNIVERSITY OF READING
Department of Mathematics, Meteorology & Physics

# The Influence of the Agulhas leakage on the overturning circulation from momentum balances

**Amandeep Virdi**

August 2010

This dissertation is submitted to the Departments of Mathematics and Meteorology in partial fulfilment of the requirements for the degree of Master of Science

## Declaration

I confirm that this is my own work, and the use of all material from other sources has been properly and fully acknowledged.

Signed: .....

Dated: .....

# Acknowledgements

*I would like to take this opportunity to thank all my family for their forever love and devotion, particularly my parents. I would not be in this position at this moment in time without them. A special thank you goes to my aunt and uncle for having me for the entire year and coping with me, especially during some intense academic times. I would like to thank my supervisor, Profesor Peter Jan van Leeuwen, for his continued support and guidance. His sublime knowledge of the subject has helped me gain an extensive understanding of this area of study and enjoy everything I have learnt so far. I would like to thank Dr Peter Sweby for giving me the opportunity to undertake this course and to prove my academic abilities. Finally I would like to express my gratitude to the Natural Environmental Research Council (NERC) for their encouragement and belief in this subject area together with the provision of their financial sponsorship.*

# Abstract

We want to investigate the influence of Agulhas rings on the ocean circulation in the South Atlantic, and so on the Overturning Circulation. The Agulhas leakage between the South Atlantic and Indian Ocean is an interocean exchange transporting heat and salt from one basin to the other. The study incorporates use of momentum and vorticity balances in order to explain the impact of Agulhas rings on the Overturning Circulation. These rings are shed in the South Atlantic and alter the momentum balance in this ocean basin. The normal occurrence is geostrophic balance, but we find an additional advection contribution in the balance. Allowing Agulhas rings to enter the basin, it becomes evident that the vorticity balance changes in comparison to a closed basin where we have no rings shed. This directly infers that the rings do have a significant influence on the circulation in the South Atlantic, and thus potentially on the Overturning Circulation.

# Contents

# List of Figures

# 1 Introduction

The Overturning Circulation or the ocean's Thermohaline Circulation is the large scale ocean circulation driven by surface heat and freshwater fluxes. W. S. Broecker (1991) describes the salt being "left behind as the result of water-vapour transport in the atmosphere from the Atlantic to the Pacific basin." He called the Overturning Circulation as The Great Ocean Conveyor.

The major importance of the Overturning Circulation is its impacts on our global climate and possibly its radiation budget. A shutdown of the conveyor has been linked to glacial periods in the past. Current climate change theory believes that increased atmospheric warming due to greenhouse gas emissions and aerosols are to increase freshwater fluxes and possibly shutdown the conveyor.

The Thermohaline Circulation is influenced by heat and salt transport that is largely brought about by ocean currents and ocean rings. Due to this, a strong interaction exists between the dynamics and the thermodynamics of the ocean. One of the main challenges presented to us in Oceanography is to understand how these two interact.

Our area of study is the South Atlantic Ocean. We know that in the Agulhas area of South Africa, large ocean rings are shed into the South Atlantic. The Agulhas leakage provides a direct interocean link between the South Atlantic and Indian Oceans. The ocean rings here are known as Agulhas rings and are shed from the retroflecting Agulhas Current. Figure 1 shows the area of study we are interested in.

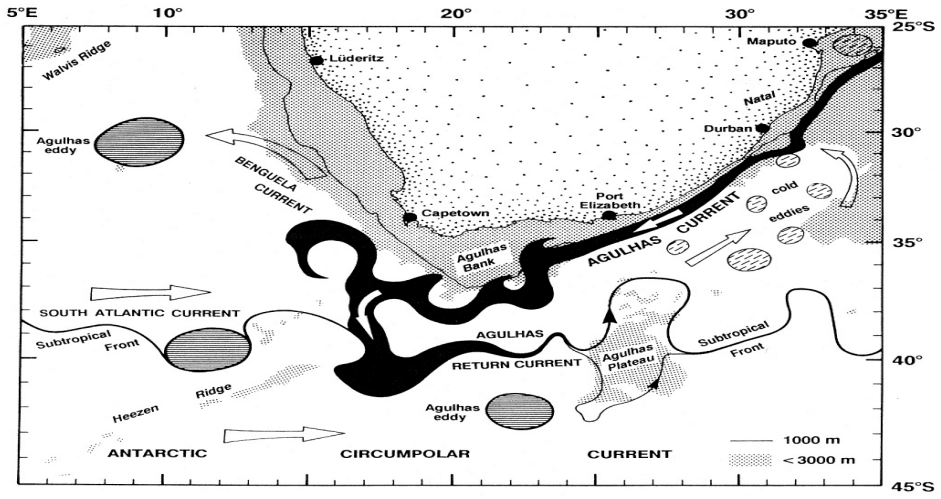


Figure 1: Image taken from Peterson and Stramma (1991) showing the Agulhas leakage into the South Atlantic Ocean.

A. L. Gordon (1985) has shown that the Indian Ocean surface water is more than 5°C warmer and has a richer salt content than the South Atlantic, approximately 0.3-0.4 practical salt units (psu) higher. These Agulhas rings transport water from the Indian Ocean into the South Atlantic which can have a major influence on the Thermohaline Circulation.

We will study the interaction between the dynamics and thermodynamics of the ocean, by investigating the momentum and vorticity balances in a reduced gravity model of the South Atlantic. This will contribute to our understanding of the Thermohaline Circulation.

By integrating the momentum and vorticity equations over an ocean basin with either closed or open boundaries, we study the relation between the wind-stress input, via the dynamics, and the behaviour of the thermocline.

The idea is to systematically study momentum and vorticity balances over the South Atlantic basin. We start with a closed basin, then move onto an open basin that gradually becomes more complicated and will eventually build up to the full problem.

Firstly, we will look at the integrated momentum equations and vorticity equation solely on the closed basin, looking at the subtropic gyre contained within it. We expect to learn something about the balances that include the information about the height profile. We expect the vorticity balance can provide a greater understanding of the physical aspects of the ocean circulation. We will then run a numerical model of the closed basin circulation and try to confirm the findings from our analytical calculations of the momentum balances.

We will then apply the momentum equations to the same South Atlantic basin implementing different boundary conditions. These boundary conditions will create an open basin. Starting with open, north and south boundaries, we will look at different situations that we expect to see in the real world, where ocean currents may enter and leave the basin. We then open the eastern boundary to allow the Agulhas leakage to enter and finally put them all together to configure what we have realistically.

With a realistic situation set up, we will use the momentum balances to aid our understanding of the effects of the Agulhas and other currents flowing into the South Atlantic, which include the Antarctic Circumpolar Current (ACC) and Malvinas Current.

We will again look at the numerical model of the South Atlantic Ocean. The model continues to examine the closed basin configuration and will focus on the vorticity balance. We will then modify the model to become an open basin in which the

Agulhas leakage is present in the basin. Using the numerical model, we aim to obtain a visual understanding of the Agulhas leakage in the ocean basin. We then have the ability to numerically calculate terms in the vorticity equation for both cases and distinguish a vorticity balance for both cases.

Studying the momentum equations and vorticity equation on the South Atlantic Ocean, using analytical and numerical methods, will give us an insight to what influence the Agulhas leakage has on the ocean basin as well as the global Overturning Circulation.

# 2 The Governing Equations

The governing equations of motion examined are the momentum equations for incompressible fluids. The current is assumed to be in steady state and a two layer, reduced gravity model is proposed. Figure 2 below shows an idealistic two layer model.

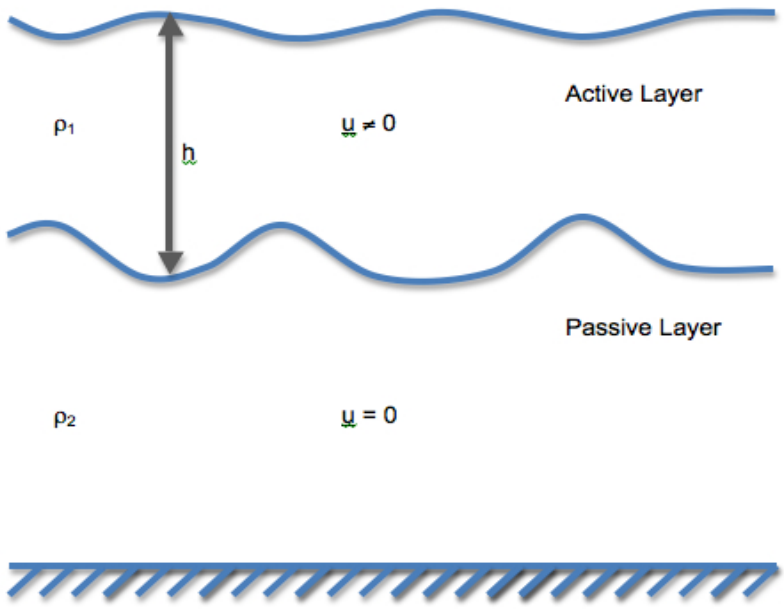


Figure 2: A two-layer ocean model with active (finite depth) and passive (infinite depth) layers.

The momentum equations in the active layer are given by

$$u_t + uu_x + vu_y - fv + g'h_x = \frac{A}{h}\nabla \cdot (h\nabla u) + \frac{\tau^{(x)}}{\rho h} \tag{1}$$

$$v_t + uv_x + vv_y + fu + g'h_y = \frac{A}{h}\nabla \cdot (h\nabla v) + \frac{\tau^{(y)}}{\rho h} \tag{2}$$

where h is the depth of the active layer (layer thickness); u and v represent the zonal and meridional velocities respectively; f is the Coriolis parameter approximated by

the beta plane ($f = f_0 + \beta y$); g′ is the reduced gravitational acceleration given by $g' = g\frac{\rho_2 - \rho_1}{\rho_1}$; A is the coefficient of lateral friction and $\tau$ is the surface wind stress.

The final equation which makes up the reduced gravity model is the continuity equation given by

$$h_t + (hu)_x + (hv)_y = 0. \tag{3}$$

Assuming steady state implies that $u_t = v_t = h_t = 0$.

The steady state continuity equation is given by

$$(hu)_x + (hv)_y = 0. \tag{4}$$

Upon multiplying (1) and (2), in steady state, by $h$ and combining them with (4), we find the momentum equations reduce to

$$(hu^2)_x + (huv)_y - fhv + \frac{1}{2}g'(h^2)_x = A\nabla \cdot (h\nabla u) + \frac{\tau^{(x)}}{\rho} \tag{5}$$

$$(huv)_x + (hv^2)_y + fhu + \frac{1}{2}g'(h^2)_y = A\nabla \cdot (h\nabla v) + \frac{\tau^{(y)}}{\rho} \tag{6}$$

where the meridional wind-stress, $\frac{\tau^{(y)}}{\rho}$ will be ignored from now on.

Analytical calculations will be used to used to evaluate equations (5) and (6). We will integrate them over a given area which will be our basin, the South Atlantic Ocean. Writing the momentum equations as (5) and (6) allows us to integrate the terms with less difficulty by the application of Stoke's theorem. We can then estimate the terms at both limits in the integral. We expect by integrating the momentum equations, to find out what terms dominate and hence what sort of balance is occurring. Furthermore, we would like to know what this tells us about our basin.

Taking our attention away from the momentum equations, we will also look at the vorticity equation. Vorticity is a local measure of rotation in a fluid. It is a measure of the spin of fluid parcels. In 2-dimensions, vorticity is defined by $\zeta = v_x - u_y$. We derive the vorticity equation by writing the momentum equations as

$$u_t + uu_x + vu_y - fv = -g'h_x + \frac{A}{h}\left[(hu_x)_x + (hu_y)_y\right] + \frac{\tau^{(x)}}{h\rho} \tag{7}$$

$$v_t + uv_x + vv_y + fu = -g'h_y + \frac{A}{h}\left[(hv_x)_x + (hv_y)_y\right]. \tag{8}$$

Taking the curl of these equations, i.e. $\frac{\partial}{\partial x}$(8) - $\frac{\partial}{\partial y}$(7) gives

$$\begin{aligned} \zeta_t &+ u\zeta_x + v\zeta_y + (f+\zeta)(u_x + v_y) + \beta v = -\left(\frac{\tau^{(x)}}{h\rho}\right)_y \\ &+ A(\zeta_{xx} + \zeta_{yy}) + A\left[\left(\frac{h_x v_x}{h}\right)_x + \left(\frac{h_y v_y}{h}\right)_y - \left(\frac{h_x u_x}{h}\right)_x - \left(\frac{h_y u_y}{h}\right)_y\right]. \end{aligned} \tag{9}$$

We multiply (9) by h and use continuity (3), to give the Vorticity Equation (10)

$$\begin{aligned} (h\zeta)_t &+ (hu\zeta)_x + (hv\zeta)_y + h(f+\zeta)(u_x + v_y) + \beta hv = -h\left(\frac{\tau^{(x)}}{h\rho}\right)_y \\ &+ hA(\zeta_{xx} + \zeta_{yy}) + hA\left[\left(\frac{h_x v_x}{h}\right)_x + \left(\frac{h_y v_y}{h}\right)_y - \left(\frac{h_x u_x}{h}\right)_x - \left(\frac{h_y u_y}{h}\right)_y\right]. \end{aligned} \tag{10}$$

In the South Atlantic Ocean, we know that rings are shed from the Agulhas leakage. The vorticity equation is useful, since we can measure the spin induced from these rings as well as other vortices that are formed. We aim to find out what effect they have on the vorticity equation. With analytical calculations and a numerical model, described in Section 3, we hope to find out what influence the Agulhas leakage has on the Overturning Circulation.

# 3 Numerical Model

Using the two layer model proposed earlier, we will be using a numerical model of the South Atlantic Ocean basin. This aims to provide a detailed picture and view of the circulation in the basin. Analytical calculations cannot provide us with detail of the circulation within the basin.

Although numerical modelling cannot output the real situation perfectly, they are increasingly becoming on par with them. As our understanding of these situations improve, they are beginning to play a more dominant role. Both time and space parameters are important in numerical modelling. We are able to calculate what time step is best for the model without it blowing up. Our analytical calculations are assumed to be in steady state which means there are no time variations. Using our numerical model, we are able to accomplish outputs that are based on time-averaged flow. These outputs provide us with a useful picture of what is occurring within the basin.

The form of the equations we are going to discretise are slightly different to the equations given in Section 2. Writing equations (1) and (2) as the equations given in (11) and (12) makes sure potential vorticity is conserved in the absence of friction.

The equations that we discretise in the numerical model are given by

$$u_t + \frac{1}{2}(u^2 + v^2)_x - (\zeta + f)v = -g'h_x + A\left(u_{xx} + u_{yy}\right) + \frac{\tau^{(x)}}{h\rho} \tag{11}$$

$$v_t + \frac{1}{2}(u^2 + v^2)_y + (\zeta + f)u = -g'h_y + A\left(v_{xx} + v_{yy}\right). \tag{12}$$

Note the different forms for friction. These are not identical but both have a sound physical basis. The details will not be discussed here. The analytical form for friction has its advantages for analytical derivations.

These equations are discretised using a Leapfrog scheme, with an initial Euler step. The Leapfrog scheme can develop an unphysical, numerical mode, that itself is stable but the solution is wrong. In order to damp this computational mode, we employ an Euler step every $16^{th}$ time-step. We discretise the equations on a 2-dimensional staggered grid known as the Arakawa-C grid. The boundary conditions given are no-slip boundary conditions in which $u$ and $v$ are both zero on all boundaries.

The time and space parameters used in the model are specifically chosen to guarantee convergence. The Courant-Friedrichs-Lewy (CFL) condition is a necessary condition which tells us the upper limit for a time-step to be used in the model.

The CFL condition is given by $\Delta t < \frac{\Delta x}{c}$, where $\Delta t$ is the time-step, $\Delta x$ is grid spacing and $c$ is the velocity of the fastest wave, which is the reduced gravity wave here.

Our model has a grid spacing, $\Delta x = 1000$ m. This value is chosen to be eddy-permitting. We know for that for gravity waves, $c = \sqrt{g'h} = 3.16\ ms^{-1}$. This gives us an upper bound for the time-step which is 316 $s$. In order to keep to this CFL condition, we take a time-step, $\Delta t = 225\ s$.

In terms of running the model, we look at the baroclinic Rossy waves travelling across the ocean basin. For these Rossby waves, $c = \beta R_d^2$, where $R_d$ is the Rossby radius of deformation, this is the characteristic length-scale for eddy generation. These Rossby waves give us $R_d = \frac{\sqrt{g'h}}{|f_0|} = 32\ km$. So we resolve at this scale; a higher resolution would be ideal but becomes too expensive to run. The numerical model has a zonal length scale $L_{nm} = 2000\ km$. We now get a minimum run time of model, $T$ which is given by $T = \frac{L_{nm}}{c} = 9.7 \times 10^7\ s \approx 3$ years. After this time, the model reaches a statistical equilibrium. We exclude the time prior to this because the idea is that the flow is turbulent and we study the time-averaged flow.

The numerical model parameters are: $g' = 0.02\, ms^{-2}$, $f_0 = -10^4\, s^{-1}$, $\beta = 2 \times 10^{-11}\, m^{-1}s^{-1}$, $A = 500\, m^2s^{-1}$ and finally $h = e + H$, where $H = 500\, m$. The variable, $e$, is the displacement of the interface, measured in meters; positive values are taken to be vertically down. A typical output of the model is shown in Figure 3.

The two basins are of identical size, connected through an opening. This is south of an island that creates boundary between the two basins, as seen in Figure 4. The left and right basins represent the South Atlantic and Indian oceans, driven by a zonal, surface wind-stress taken as $0.1\, Pa$ and $0.2\, Pa$ respectively. These are chosen representing yearly averaged values and can be amended. We see after a 1000 day run, Figure 3, that the displacement of the interface $e$, is deeper close to western boundaries but not on the boundaries themselves. Where the wind-stress is stronger in the Indian Ocean, we notice that the layer is also deeper here in comparison to the South Atlantic.

Due to the open island, we are able to see the model's eddy permitting behaviour. We can see eddies moving into the South Atlantic basin. These eddies cause a change in the layer depth and each vary in height. The output shown is a snapshot of the ocean at a given time of 1000 days and provides us with an idea of what the active layer is doing given the setup.

The numerical model will be used to confirm findings generated by the momentum equations and to look at the vorticity within the basin. As well as numerically modelling the basin, we will use the model to numerically calculate terms in the vorticity equation, that are time-averaged and look at how it is balanced.

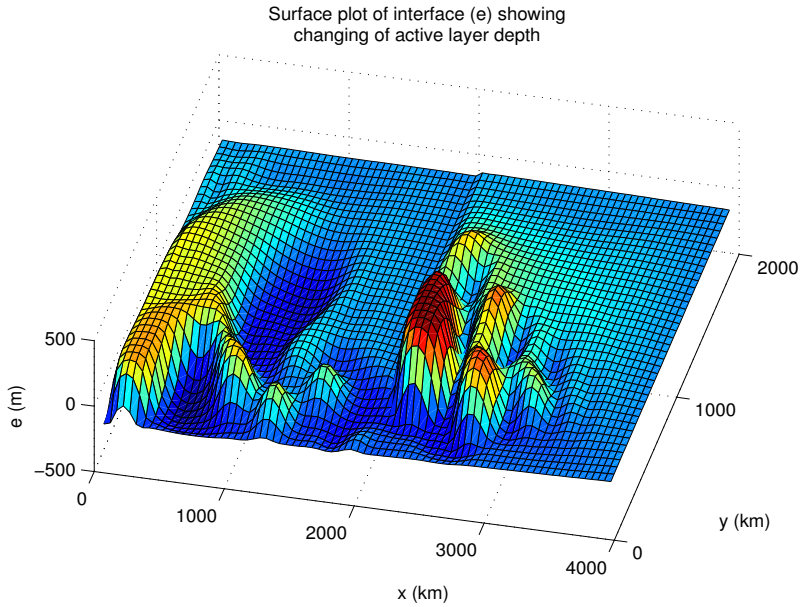


Figure 3: Plot showing output of model when run for 1000 days.

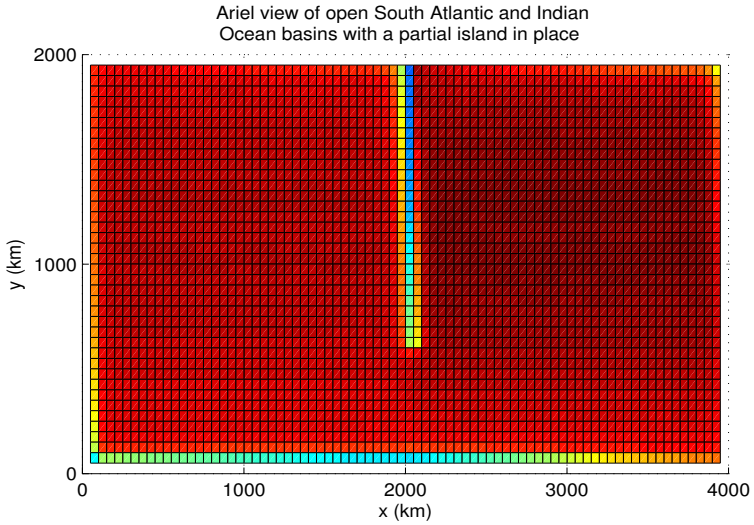


Figure 4: Plot of the island used in the numerical model.

# 4 Application on a Closed Basin

Firstly, we apply the momentum equations on a closed basin, where $u = 0$ on the eastern and western boundaries and $v = 0$ on the northern and southern boundaries. This closed basin encloses an anticyclonic wind-driven gyre with strongest current along the western boundary.

Throughout we will use the Cartesian coordinate system, taking $x$ along the zonal and $y$ along the meridional direction. The basin we use has an area $\phi$ that has length scales $x = L$ and $y = M$, where $L = 5,000\ km$ and $M = 2,000\ km$. Our aim is to mimic the South Atlantic Ocean.

Figure 5 shows a diagram of the closed basin and a typical gyre that we will be examining. The diagram tries to depict the fact that the western boundary current, flowing southwards is a narrow, fast-flowing current. The rest of the gyre flows slower and typically is a lot wider than the western boundary current.

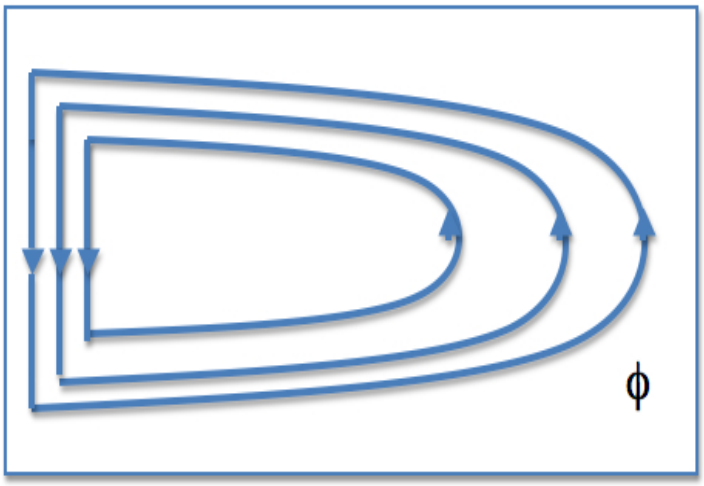


Figure 5: Anticyclonic Gyre Within a Closed Basin.

## 4.1 The Zonal Momentum Equation

The zonal momentum equation is what we examine first and foremost. We begin by using Stoke's theorem and integrating (5) over the closed basin $\phi$, i.e.

$$\iint_{\phi} \left[ (hu^2)_x + (huv)_y - fhv + \tfrac{1}{2} g'(h^2)_x - A\nabla \cdot (h\nabla u) - \tfrac{\tau^{(x)}}{\rho} \right] dx\, dy = 0$$

$$\implies \int huv\Big|_{y=0}^{y=M} dx + \int \left[(hu^2) + \tfrac{1}{2}g'(h^2)\right]_{x=0}^{x=L} dy$$
$$- \iint \left[fhv + A\nabla\cdot(h\nabla u) + \tfrac{\tau^{(x)}}{\rho}\right] dx\,dy = 0.$$

We know that $u = 0$ on the eastern and western boundaries and $v = 0$ on the northern and southern boundaries so the first and second terms vanish. We expect that these do vanish because they are the advection terms and on a closed basin we should find no advecting mass on the boundaries. Furthermore, since the basin is closed, we cannot introduce any new mass into the basin. This means that there can be no other advection so these terms should always remain zero.

So we are left with

$$\int \tfrac{1}{2}g'[h^2]_{x=0}^{x=L}\,dy - \iint [fhv + A\nabla\cdot(h\nabla u) + \tfrac{\tau^{(x)}}{\rho}]\,dx\,dy = 0.$$

Equation (4) allows us to introduce a transport stream function by $hu = -\psi_y$ and $hv = \psi_x$. Indeed, if substitute these into (4) gives us $-\psi_{xy} + \psi_{xy} = 0$, where we call $\psi$ a stream function. Integrating the stream function in the zonal direction gives us

$$\int_0^L \psi_x\,dx = \int_0^L hv\,dx$$
$$\implies \psi(L) - \psi(0) = \int_0^L hv\,dx.$$

The stream function measures the transport. The amount of water flowing northward in the interior of the basin is equal to the amount flowing southward along the western boundary. This tells us that

$$\psi(L) - \psi(0) = \int_0^L hv\,dx = 0.$$

Using what we know about the stream function, we can now rewrite the Coriolis term as

$$-\iint fhv\,dx\,dy = \iint -f\psi_x\,dx\,dy = -\int f[\psi]_{x=0}^{x=L}\,dy = 0.$$

We find that the Coriolis force has no effect on the closed basin in the zonal direction.

This now leaves us with

$$\int \tfrac{1}{2}g'[h^2]_{x=0}^{x=L}\,dy = \iint \left[A\nabla\cdot(h\nabla u) + \tfrac{\tau^{(x)}}{\rho}\right] dx\,dy.$$

The first term on the right hand side of the equation, the friction term, can be written as

$$-\iint A\nabla\cdot(h\nabla u)\,dx\,dy = -\iint A[(hu_x)_x + (hu_y)_y]\,dx\,dy$$
$$= -A\int hu_x\Big|_{x=0}^{x=L}\,dy - A\int hu_y\Big|_{y=0}^{y=M}\,dx.$$

The second term on the right hand side is the wind stress. The wind stress is assumed to be given by $\tau^{(\mathbf{x})} = \left(-\tau_0 cos\left(\frac{y\pi}{M}\right), 0\right)$. When integrated over the whole basin, this term is zero, i.e.

$$\iint \frac{\tau^{(x)}}{\rho}\,dx\,dy = -\iint \frac{1}{\rho}\tau_0 cos(\tfrac{y\pi}{M})\,dx\,dy = -\int \frac{1}{\rho}\tau_0\frac{M}{\pi}sin(\tfrac{y\pi}{M})\Big|_{y=0}^{y=M}\,dx = 0.$$

The three remaining terms in the equation which are left to evaluate are

$$\int \tfrac{1}{2}g'[h^2]_{x=0}^{x=L}\,dy - A\int hu_x\Big|_{x=0}^{x=L}\,dy - A\int hu_y\Big|_{y=0}^{y=M}\,dx = 0.$$

We estimate the terms by using Scale Analysis where we estimate the magnitude of each individual term.

Table 1 gives a list of the all the terms used and their approximate values when applied to the oceanic circulation in the South Atlantic Ocean.

| Variable | Magnitude | Symbol |
|---|---|---|
| $h$ | 500 $m$ | $H$ |
| $u$ | 0.01 $ms^{-1}$ | $U$ |
| $v$ | 0.01 - 1 $ms^{-1}$ | $V$ |
| $f_0$ | $-10^{-4}s^{-1}$ | $f_0$ |
| $\beta$ | $2\times10^{-11}\ m^{-1}s^{-1}$ | $\beta$ |
| $g'$ | 0.02 $ms^{-2}$ | $g'$ |
| $A$ | 100 $m^2s^{-1}$ | $A$ |
| $\tau_0$ | 0.1 $Pa$ | $\tau_0$ |
| Width of the current (zonal direction) | 100 $km$ - 1000 $km$ | $L_x$ |
| Width of the current (meridional direction) | 1000 $km$ | $L_y$ |
| Basin width (east-west) | 5000 $km$ | $L$ |
| Basin length (north-south) | 2000 $km$ | $M$ |

Table 1: Orders of magnitude of reduced gravity model terms

The frictional terms are trickier to evaluate. We must take into account the velocity of the current at the boundary as well as the width of the current. They are approximated as follows

$$-A\int hu_x\Big|_{x=0}^{x=L}\,dy - A\int hu_y\Big|_{y=0}^{y=M}\,dx$$
$$\approx -AH\left(\tfrac{U}{L_x}|_{x=L} - \tfrac{U}{L_x}|_{x=0}\right)M - AH\left(\tfrac{U}{L_y}|_{y=M} - \tfrac{U}{L_y}|_{y=0}\right)L \approx 5000\ m^4s^{-2}.$$

Note that we are using the coordinate system such that water flowing eastwards has a positive value for $u$ and is negative for water flowing westwards.

Using the total contribution which is just the friction term, we can find the pressure term. This means that

$$\int \tfrac{1}{2} g' [h^2]_{x=0}^{x=L} \, dy = -5000 \, m^4 s^{-2}$$
$$\implies [h^2]_{x=0}^{x=L} = -0.25 \, m^2.$$

Showing us that the difference here must be small. This tells us something about the height profile at each of the boundaries at $x = 0$ and $x = L$. Since the pressure term must balance the momentum equation in the zonal direction and the integral must be small, the depth of water must be similar at both boundaries.

If we take the integral, $\int \frac{1}{2} g' [h^2]_{x=0}^{x=L} \, dy$, the only way this can be small is if the integral evaluated at each limit equals each other. In other words

$$\int \tfrac{1}{2} g' [h^2]_{x=L} \, dy = \int \tfrac{1}{2} g' [h^2]_{x=0} \, dy.$$

So this tells us that $h(x{=}L) \approx h(x{=}0)$. The depths are about equal at both the east and west boundaries.

## 4.2 The Meridional Momentum Equation

We now look at the meridional momentum equation, equation (6). In a similar manner, we integrate over the closed basin $\phi$ and apply Stoke's theorem to this equation. We get the following

$$\iint_{\phi} \left[ (huv)_x + (hv^2)_y + fhu + \tfrac{1}{2} g' (h^2)_y - A \nabla \cdot (h \nabla v) \right] dx \, dy = 0.$$

Both the advection terms are zero since we know that for a gyre in this closed basin $u = 0$ on the eastern and western boundaries and $v = 0$ on the northern and southern boundaries. As mentioned in the zonal momentum equation previously, we expect that the advection are zero on the closed basin. There is also no wind stress in this direction. We are left with

$$\iint_{\phi} \left[ fhu + \tfrac{1}{2} g' (h^2)_y - A \nabla \cdot (h \nabla v) \right] dx \, dy = 0.$$

We saw previously how we can write the friction term and we get the following

$$\iint_{\phi} [fhu + \tfrac{1}{2} g' (h^2)_y] \, dx \, dy - \int A h v_x \Big|_{x=0}^{x=L} \, dy - \int A h v_y \Big|_{y=0}^{y=M} \, dx = 0.$$

We estimate the Coriolis term by splitting the basin into two halves, due to the strength of this term varying with latitude and the zonal velocity having a sign change. Furthermore, we approximate the Coriolis parameter using the Beta approximation, where $f = f_0 + \beta y$. It is estimated as follows

$$\iint_{\phi} fhu\,dx\,dy = \iint (f_0 + \beta y)hu\,dx\,dy = \iint \beta yhu\,dx\,dy.$$

The term $\iint_{\phi} f_0 hu\,dx\,dy = 0$ since we know that the mass transport in the northern half of the basin is equal to the amount flowing in the southern half of the basin and $f_0$ is a constant, similar to the situation in the zonal case when we looked at the stream function. Noting that $u$ has a sign change halfway in the basin, we are left with

$$\iint \beta yhu\,dx\,dy = \beta HU \int \left[ \int_0^{M/2} y\,dy - \int_{M/2}^{M} y\,dy \right] dx$$

$$\implies \tfrac{1}{2}\beta HU \int \left[ (M/2)^2 - (M^2 - (M/2)^2) \right] dx = -\beta HU \tfrac{M^2}{4} L \approx -5 \times 10^8\ m^4 s^{-2}.$$

The frictional terms are

$$-\int Ahv_x \Big|_{x=0}^{x=L} dy - \int Ahv_y \Big|_{y=0}^{y=M} dx \approx$$

$$-AH\left(\tfrac{V}{L_x}|_{x=L} - \tfrac{V}{L_x}|_{x=0}\right) M - AH\left(\tfrac{V}{L_y}|_{y=M} - \tfrac{V}{L_y}|_{y=0}\right) L \approx -1 \times 10^6\ m^4 s^{-2}.$$

We notice that the frictional term arising from the western boundary current is much larger in the meridional direction compared to the zonal direction.

Thus the dominating term is the Coriolis term and we find the only way this can be balanced is by the pressure term. The pressure term, $\iint_{\phi} \frac{1}{2} g' (h^2)_y\,dx\,dy$, must be of equal magnitude to the Coriolis term, but opposite in sign.

We find that the by the orders of magnitude estimates of the terms, that there is now a balance between the Coriolis and pressure forces. This tells us that the depth of water in the closed basin setup is deeper nearer to the equator at the northern boundary and shallower at the southern boundary. We know this is the case by looking at the pressure term and its sign. The difference between the pressure at the northern boundary and the southern boundary has to be positive. We can see this by

$$\iint_{\phi} \tfrac{1}{2} g' (h^2)_y\,dx\,dy = \int \tfrac{1}{2} g' [h^2]_{y=0}^{y=M}\,dx = 5 \times 10^8\ m^4 s^{-2} > 0$$

$$\implies \int \tfrac{1}{2} g' [h^2]_{y=M} - \int \tfrac{1}{2} g' [h^2]_{y=0} > 0$$

$$\implies \int \tfrac{1}{2} g'[h^2]_{y=M} > \int \tfrac{1}{2} g'[h^2]_{y=0}.$$

The only solution is that the water is deeper north of the basin and shallower south of the basin. See Figure 6 below.

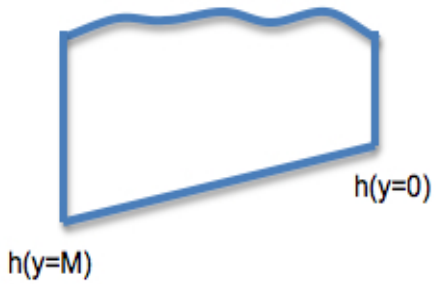


Figure 6: Typical depth profile in the meridional direction.

## 4.3 Numerical Model Verification

The analytical results of the momentum balances in the zonal and meridional tell us about the height profile of the basin using a two-layer model. We now wish to confirm the results using our numerical model.

Running the numerical model until a statistical equilibrium is reached allows us to compare our numerical results to our analytical calculations. This is achieved after approximately 1000 days.

The average depths at the boundaries of the closed basin we find from the numerical model are given in Table 2. We must be careful here as the numerical model outputs a value for the elevation, $e$, above our active layer, $H$, taken to be $500\,m$. The depth is calculated by $h = e + 500$. The model uses the elevation throughout so we must remember to add the active layer depth to find our depth values.

| | N | S | E | W |
|---|---|---|---|---|
| $h$ | 480 m | 460 m | 468 m | 469 m |

Table 2: Average Depth Profile at Boundaries of the Closed Basin

We find that the numerical model confirms our analytical findings. The northern boundary has a deeper averaged height profile than the southern boundary. We also find that the averaged depth at the eastern boundary is almost equal to the western boundary.

## 4.4 Estimating the Vorticity Equation on the Closed Basin

We now move onto the vorticity equation. We will again integrate the equation on the closed basin $\phi$ and estimate each of the terms to see what sort of vorticity balance we find.

Firstly, we assume steady state, so the time dependent term, $(h\zeta)_t = 0$.

Since we are looking at the closed basin, the boundary conditions mean that the advection terms are zero. So

$$\iint \Big[(hu\zeta)_x + (hv\zeta)_y\Big]\, dx\, dy = 0.$$

We now wish to estimate the stretching term. We use our knowledge of geostrophic balance to provide us with a useful relationship. The geostrophic equations are written

$$fv = g'h_x \tag{13}$$

$$fu = -g'h_y. \tag{14}$$

Taking the curl of the above equations, i.e. $\frac{\partial}{\partial x}$(14) - $\frac{\partial}{\partial y}$(13) gives us

$$f(u_x + v_y) + \beta v = 0.$$

An alternative explanation to this comes from the individual terms. We expect that the terms such as $fv_y$ and $\beta v$ are relatively large due to the faster meridional velocities within the basin, for instance in the western boundary current. However, the terms here tend to cancel with one another making it difficult to estimate the stretching term. We note that in this approximation, we have ignored the $\zeta$ term. We can do this because our approximation of $|f| = 10^{-4}s^{-1}$ and $|\zeta| \approx 10^{-9}s^{-1}$ in the interior of the basin, where $\zeta = v_x - u_y \approx \frac{V}{L} - \frac{U}{M} \approx -3 \times 10^{-9}s^{-1}$.

The maximum value $\zeta$ can possibly take is in the western boundary current and this is approximately $\zeta = \frac{V}{L} \approx \frac{-1}{10^5} = -10^{-5}s^{-1}$. We notice that, throughout the closed basin, $|f| > |\zeta|$. Hence, we can ignore $\zeta$ in the stretching term. We find that the stretching term now cancels due to the geostrophic relationship, as a first guess.

We now turn to the right hand side of the vorticity equation and estimate the terms. The vorticity input by wind term over the whole basin is approximated as follows

$$\iint -h\left(\frac{\tau^{(x)}}{h\rho}\right)_y \, dx\, dy \approx -H\frac{\tau^{(x)}}{H\rho M}LM = -\frac{\tau^{(x)}}{\rho}L.$$

The wind stress over the basin is has an approximate value of $\tau^{(x)} = 0.1Pa$ and the density $\rho = 1024\ kgm^{-3}$.

So this leaves us with

$$\iint -h\left(\frac{\tau^{(x)}}{h\rho}\right)_y \, dx\, dy \approx -\frac{\tau^{(x)}}{\rho}L \approx 500\ ms^{-2}.$$

We now move onto the friction terms. We begin by looking at the terms given by

$$\iint hA(\zeta_{xx} + \zeta_{yy})\, dx\, dy.$$

This term will be largest at the western boundary, where we have the strong western boundary current. This current is located on our coordinate system at $x{=}0$. A good estimate will be found if we approximate this term here, hence we only need to look at the term depending on $x$. The magnitude of the term depending on $y$ should be no larger than this term.

We find that the magnitude is given by

$$\iint hA(\zeta_{xx} + \zeta_{yy})\, dx\, dy \approx \iint hA\zeta_{xx}\, dx\, dy$$
$$\approx \int_0^M hA[\zeta_x]_0^L\, dy \approx -\int_0^M hA\zeta_x(x=0)\, dy \approx -HA\frac{V}{L_1^2}M = 10\ ms^{-2}.$$

The final four terms in the vorticity equation have a similar magnitude to the previous two friction terms. If we look at the magnitude of the one of the terms that we believe will be largest we have

$$\iint hA\frac{h_x v_x}{h}_x \, dx\, dy = \int hA\frac{h_x v_x}{h}\, dy \approx HA\frac{HV}{HL^2}M.$$

This is very similar to the magnitude of the friction term done previously. So these terms collectively must be of order of magnitude $10\ ms^{-3}$.

This ultimately tells us one thing about the vorticity in the gyre. The coefficient of lateral friction or diffusivity term, A, must be an order of ten larger than what we have estimated it to be. We had taken $A = 100\ m^2s^{-1}$ but for the vorticity equation to balance, it must be ten times larger, say $A = 1000\ m^2s^{-1}$.

Physically, this means that the ocean is not in steady state. Taking $A = 100\ m^2s^{-1}$, is a commonly chosen number for an ocean in steady state, but as we have just found, in some cases it will be different.

The ocean not being in steady state means that time variations are important. To correct this, we use a method of averaging. Averaging the terms over time allows us to take time into account under turbulent conditions.

A method used to do this is called Reynolds Averaging. This is where turbulent fluctuations are separated from the mean flow. It lets us average terms in time.

In order to do this we write our variables as a time-averaged part and a time-varying part, for example

$$u = \overline{u} + u'$$
$$v = \overline{v} + v'$$
$$h = \overline{h} + h'.$$

Without going over the details here, a time evaluated integral is completed and we get the following,

$$\frac{1}{T}\int_0^T (huv)_x \, dt = \overline{h}\,\overline{u}\,\overline{v} \; + \text{other terms},$$

where the other terms include Reynolds averaged terms.

We find that the terms in this integral, contribute to something physical in the basin. This is known as eddy diffusion. Eddy diffusion comes about from the time-averaging process via the Reynolds terms and becomes apparent when we have turbulent motion. Averaging in time shows this eddy diffusion happening. This is the reason for why the diffusivity, $A$, has to become larger. The tenfold increase of $A$ compensates for eddy diffusion.

When looking at the momentum equations, we have ordinarily taken the diffusivity, $A = 100\, m^2 s^{-1}$. However, we have just found that for the values used in the vorticity equation, $A$ must be approximately ten times larger.

This now effects the friction terms in both the zonal and meridional directions. We find that even with an increase of $A$, the friction terms do not contribute to the momentum balance we found previously. Noticeably, the meridional momentum equation now has its friction term with an order of $10^7\, m^4 s^{-2}$. However, the pressure and Coriolis terms remain dominant in this equation.

# 5 Application on an Open Basin: Open North and South Boundaries

In the next section, we examine the case discussed previously but this time the northern and southern boundaries are now open. This leads to a volume flux entering at the southern boundary, near the western edge and leaving at the northern boundary.

## 5.1 Scenario 1: Southern Inflow and Northern Outflow

Our first case of an open basin is where we look at mass transport entering the gyre at the southern end next to the western boundary and leaving at the northern end next to the same boundary. This situation can be viewed in Figure 7.

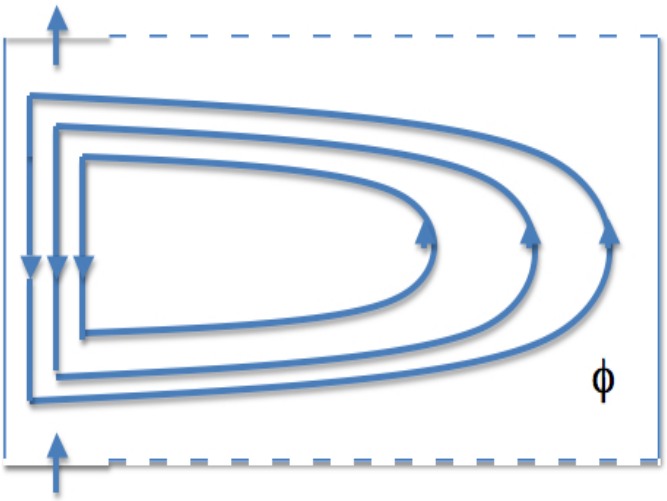


Figure 7: Anticyclonic Gyre Within an Open Basin: First Scenario.

With the Thermohaline Circulation in mind, entering the basin is approximately 15 $Sv$ ($1\,Sv \equiv 10^6 m^3 s^{-1}$) of mass transport and this is the same leaving the basin. This corresponds to a velocity $v_1 = 0.3\ ms^{-1}$. The orders of magnitude for the rest of the terms are again as in Table 1, in Section 4. Furthermore, we must note that the velocity entering and leaving the basin does so over a space scale of $L_1 = 100$ km, i.e. representing a narrow current.

We are able to show these estimates of the velocity entering the basin by using our

knowledge of mass transport, $\int_0^{L_1} hv_1\,dx \approx HV_1L_1 \approx 15 \times 10^6\, m^3 s^{-1}$, taking a depth $H \approx 500\, m$.

### 5.1.1 Zonal Momentum Equation

Integrating equation (5) and using Scaling Analysis as done previously allows us to calculate estimates for the terms in the zonal momentum equation. We find that the first advection term

$$\iint_{\phi} (hu^2)_x\,dx\,dy = 0.$$

We know this because $u$ does not penetrate through the east and west boundaries.

The second advection term is given by

$$\iint_{\phi} (huv)_y\,dx\,dy.$$

We must be careful with this advection term as when subtracting the orders of magnitudes at both limits, we can get a cancellation. This is the case when taking the in and outflow as completely northwards. However, taking a component of $u$, where $u = 0.01\ ms^{-1}$, westwards, at the northern boundary and $u = 0.01\ ms^{-1}$, eastwards, at the southern boundary then there is a momentum contribution. This will correspond to the outflow flowing very slightly to the northwest and inflow flowing very slightly to the northeast. Taking these $u$ values gives us a value for this approximation as

$$\iint_{\phi} (huv)_y\,dx\,dy = \int huv\Big|_{y=0}^{y=M} dx \approx -3 \times 10^5\ m^4 s^{-2}.$$

The Coriolis term can be approximated at mid-basin. This is valid because the value is of a similar magnitude here, compared to the northern and southern boundaries of the basin. We take $f \approx -10^4\ s^{-1}$ for a mid-basin value. Hence

$$\iint_{\phi} fhv\,dx\,dy \approx fhv_1L_1M \approx -3 \times 10^9\ m^4 s^{-2}.$$

The friction terms only depend on $u$ in the zonal case and are approximated to be

$$\iint_{\phi} -A\nabla \cdot (h\nabla u)\,dx\,dy = -\int Ahu_x\Big|_{x=0}^{x=L} dy - \int Ahu_y\Big|_{y=0}^{y=M} dx$$

$$= -\int Ahu_y\Big|_{y=0}^{y=M} dx \approx 1.5 \times 10^4 \; m^4 s^{-2}.$$

We note that the values for the current along the north and south boundaries are found using continuity, where $\int hu\,dy = 15\,Sv$, giving a value of $u = -0.03\,ms^{-1}$ in the northern half of basin. This is equal and opposite in the southern half of the basin. Furthermore, $u$ does not penetrate the east and west boundaries, so the first term vanishes.

The wind stress, as seen earlier, gives no contribution, so

$$\iint -\tfrac{\tau^{(x)}}{\rho}\,dx\,dy = 0.$$

The pressure term depends on the depth of water at the east and west boundaries. The Coriolis term dominates the momentum equation here and we know that the pressure term is the only term that can now balance the equation. We find that

$$\iint_{\phi} \tfrac{1}{2}g'(h^2)_x\,dx\,dy \approx -3 \times 10^9 \; m^4 s^{-2}.$$

We find that for this open basin, the result is the current is in geostrophic balance. This is where the Coriolis term and pressure term dominate the equation. They act in order to balance each other.

Figure 6 shows how the two forces act upon a fluid parcel, **u**.

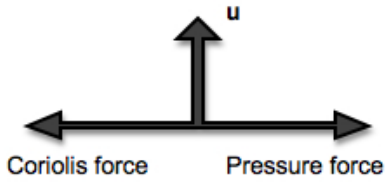


Figure 8: Geostrophic Balance.

The two forces act at a 90° angle towards the fluid parcel. The equation that governs geostrophic balance is

$$-fv = -\tfrac{1}{\rho}\tfrac{\partial p}{\partial x} = -g'\tfrac{\partial h}{\partial x}.$$

Furthermore, by looking at the orders of magnitude, we can find out the height profile at the eastern and western boundaries.

The Coriolis and pressure terms dominate the zonal momentum equation. The pressure term is negative, and we find that

$$\int \tfrac{1}{2}g'[h^2]_{x=0}^{x=L} < 0$$

which tells us that $h(x = L) < h(x = 0)$.

This situation of water flowing in at the southern entrance, around the gyre and then leaving at the northern exit gives us geostrophic balance. This fact tells us something about the depth profile in the zonal direction. We have now found that the momentum balances tell us that the layer is deeper where the water enters and leaves the basin compared to where it flows around the gyre near the eastern boundary.

This must mean that when the water flows around the gyre, it is spreading out horizontally rather than vertically. We may expect that this is due to the action of the Coriolis and pressure force balance we have in this situation. It may also be explained by the existence of the wind driven gyre, where the flow near the eastern boundary, the northward transport, is far wider than the western boundary current. This may encourage the entering water to also follow a similar width profile away from the western boundary.

### 5.1.2 Meridional Momentum Equation

We now move onto the meridional momentum equation. We estimate the terms in equation (6) and get the following

$$\iint_{\phi} (huv)_x \, dx \, dy = \int (huv)\Big|_{x=0}^{x=L} \, dy = 0.$$

The term is zero as u = 0 on the eastern boundary and u = 0 on the western boundary, as we found previously.

For the north-south advection term in the meridional case we notice that the flow entering the basin is the same as the flow leaving the basin. This gives us a cancellation, and this term is zero. So,

$$\iint_{\phi} (hv^2)_y \, dx \, dy = \int hv^2\Big|_{y=0}^{y=M} \, dx = 0.$$

The Coriolis term must be split into its beta approximation, as there is a contribution due to a difference in latitude. We recall that the mass transport in the southern half of the basin is exactly the same as the transport in the upper half of the basin. This means we get the following

$$\iint_{\phi} fhu \, dx \, dy = \iint f_0 hu \, dx \, dy + \iint \beta yhu \, dx \, dy = \iint \beta yhu \, dx \, dy.$$

For the remaining term, we split the basin into half. Upon noting the sign change of $u$ and integrating, we find that

$$\iint \beta y h u \, dx \, dy = \beta h u \int \left[ \int_0^{M/2} y \, dy - \int_{M/2}^{M} y \, dy \right] dx$$

$$\approx \tfrac{1}{2} \beta H U \int \left[ (M/2)^2 - (M^2 - (M/2)^2) \right] dx = -\beta H U \tfrac{M^2}{4} L_1.$$

The approximation of $u$ inside the basin is unknown for this situation so we use equation (4) to find an estimate.

Taking a small section of the basin, say from $x = 0$ to $x = L_1$ and $y = 0$ to $y = \frac{M}{2}$, we integrate equation (4) over this domain to find that

$$\int_0^{L_1} \int_0^{\frac{M}{2}} [(hu)_x + (hv)_y] \, dy \, dx = 0 \implies \int (hu)_{x=L_1} \, dy = \int (hv)_{y=0} \, dx.$$

Since $u$=0 on $x$=0 and $v$=0 on $y = \frac{M}{2}$, we find that $\int (hu)_{x=L_1} \, dy = \int (hv)_{y=0} \, dx$.

By using a Scale Analysis approximation we get a relationship which is given by

$$HU\tfrac{M}{2} = HV_1 L_1$$

We now have a relationship which contains our unknown approximation of $u$, so we can substitute this into our approximation of the Coriolis term to find that

$$-\beta H U \tfrac{M^2}{4} L_1 = -\beta H U \tfrac{M}{2} \tfrac{M}{2} L_1 = -\beta H V_1 L_1 L_1 \tfrac{M}{2} = -3 \times 10^7 \; m^4 s^{-2}.$$

We must remember that the wind driven gyre is also circulating and we have until now ignored the effects of this gyre. This gyre has to be included as it does have an impact on the Coriolis term. We find that the total Coriolis effect is

$$\iint_{\phi} f h u \, dx \, dy \approx -3 \times 10^7 \; m^4 s^{-2} - 5 \times 10^8 \; m^4 s^{-2} = -5.3 \times 10^8 \; m^4 s^{-2}.$$

The friction term is calculated for the inflow and outflow. These cancel with each other due to their same sign and nature. However, for the flow northwards against the eastern boundary, the approximation is given by

$$\iint_{\phi} -A \nabla \cdot (h \nabla v) \, dx \, dy \approx -3 \times 10^5 \; m^4 s^{-2}.$$

Adding the friction due to the gyre, we get the following

$$\iint_{\phi} -A \nabla \cdot (h \nabla v) \, dx \, dy \approx 3 \times 10^5 - 1 \times 10^6 = -1.3 \times 10^6 \; m^4 s^{-2}.$$

We see that the pressure term remains and for the momentum equation to balance here, this term must match the Coriolis term. So we find that

$$\iint_{\phi} \tfrac{1}{2} g'(h^2)_y \, dx \, dy \approx 5.3 \times 10^8 \; m^4 s^{-2}.$$

Now we find no contribution from the advection terms in the meridional momentum equation. This time the pressure term dominates the momentum balance along with the Coriolis term, which maintains its strength from the gyre. Once again, like the closed basin this tells us that the layer is deeper at the northern boundary since we have a balance in which its sign is positive.

So both equations give us a geostrophic relationship that relates the pressure force on a fluid parcel with the Coriolis force on the same parcel, of which they act in opposite directions.

## 5.2 Scenario 2: Southern Inflow and Southern Outflow

Our second case of an open basin is now looking at mass transport entering the gyre at the southern boundary adjacent to the western boundary. This mass transport then flows eastwards eventually leaving the basin at the southern boundary adjacent to the eastern boundary. This situation can be seen in Figure 9 below.

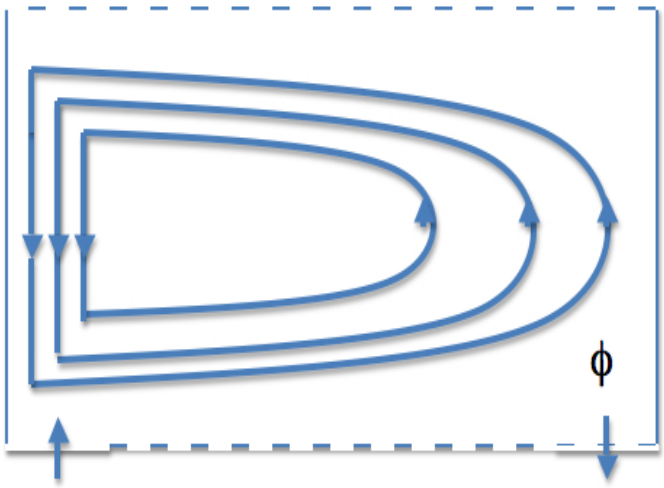


Figure 9: Anticyclonic Gyre Within an Open Basin: Second Scenario.

We use an amount of 15 Sv for the inflow and 15 Sv for the outflow. The length scale of water flowing in and out is taken to be $L_2 = 100$ km. Using our knowledge of mass transport, we can estimate the velocity of the water flowing in, and this will be the same for the water flowing out.

In the exact manner as done in the first scenario, taking $h = 500$ m, we find that

$$\int hv_2\,dx = 15\ Sv \implies HV_2L_2 \approx 15 \times 10^6\ m^3s^{-1} \implies V_2 \approx 0.3\ ms^{-1}.$$

We have the velocity, $v_2$ for the mass transport entering this will be equal but opposite for the mass transport leaving. We are now a position to estimate the momentum equation for this scenario.

### 5.2.1 Zonal Momentum Equation

The first advection term is zero due to the boundary conditions at $x = 0$ and $x = L$, i.e.

$$\iint_\phi (hu^2)_x\,dx\,dy = 0.$$

The second advection term is also zero. This is still the case if we take the inflow and outflow as not entirely meridional, say, it has a component $u = 0.01\ ms^{-1}$, flowing eastwards. The terms cancel on the southern boundary,

$$\iint_\phi (huv)_y\,dx\,dy = \int huv\Big|_{y=0}^{y=M}\,dx = -\int huv\Big|_{y=0}\,dx = 0.$$

The Coriolis parameter and the mass transport are of equal magnitude but opposite sign for inflow and outflow, so upon adding both contributions we get

$$\iint_\phi -fhv\,dx\,dy = 0.$$

The friction term integrated over the basin is also as we found earlier

$$\iint_\phi -A\nabla\cdot(h\nabla u)\,dx\,dy \approx 5000\ m^4s^{-2}.$$

Similarly to the gyre scenario in the closed basin, we find the pressure term must also be small in order to get a correct momentum balance. It must balance with the total contribution from the other terms. So we find that

$$\iint_\phi \tfrac{1}{2}g'(h^2)_x\,dx\,dy \approx 5000\ m^4s^{-2}.$$

Unlike the previous situation there is no acting Coriolis term on this flow and for this momentum equation to hold, the depth at the eastern boundary must be approximately equal to the depth at the western boundary, as found in the closed basin earlier.

### 5.2.2 Meridional Momentum Equation

Now we look at the meridional momentum equation and find approximations for the the following terms like we have seen previously.

The first advection term is zero due the boundary conditions at $x = 0$ and at $x = L$,

$$\iint_{\phi} (huv)_x \, dx \, dy = 0.$$

The second advection term now contributes since the sign of $v$ is always positive, we find that

$$\iint_{\phi} (hv^2)_y \, dx \, dy = \int hv^2 \Big|_{y=0}^{y=M} \, dx = - \int hv^2 \Big|_{y=0} \, dx \approx -9 \times 10^6 \; m^4 s^{-2}.$$

The Coriolis term is calculated using mass continuity since we do not know what the velocity $u$ is as the water flows eastwards along the southern boundary.

In Section 4.1.2, we saw the method used to approximate a value for $u$, we use the same method here, taking the same small area and find that

$$HU_2 \tfrac{M}{2} = HV_2 L_2.$$

We now estimate the Coriolis term over the southern half of the basin, where the water is flowing, and we find that

$$\iint_{\phi} fhu \, dx \, dy \approx fHU_2 L \tfrac{M}{2} = fHV_2 L_2 L \approx -7.5 \times 10^9 \; m^4 s^{-2}.$$

Since this mass transport acts in addition to the gyre within the basin, we must add the Coriolis force contribution from the gyre to give us a total contribution of $-8 \times 10^9 \; m^4 s^{-2}$.

The friction terms are first estimated for the inflow and outflow which do not cancel here, the approximation is

$$\iint_{\phi} -A \nabla \cdot (h \nabla v) \, dx \, dy \approx 3 \times 10^5 \; m^4 s^{-2}$$

Now adding the friction created by the gyre, we have a total contribution of $-7 \times 10^5 \; m^4 s^{-2}$

The pressure term over the basin in the meridional direction must balance with the Coriolis term so we find that

$$\iint_{\phi} \tfrac{1}{2} g' (h^2)_y \, dx \, dy \approx 7.5 \times 10^9 \; m^4 s^{-2}.$$

We find firstly that the meridional advection term in this equation gives us a contribution worth mentioning but the Coriolis and pressure terms are dominant and again balance the equation giving us a geostrophic balance between the two terms. This concept holds true for this flow into the basin, in this direction.

However, in the zonal equation we did not find a geostrophic balance. This can be explained by the current not having a net Coriolis contribution for the inflow and outflow. In the next scenario, when looking at a current similar to this one but where some transport is deflected northward and around the gyre, we should find the results differ due this deflection of current.

## 5.3 Scenario 3: Southern Inflow with Southern and Northern Outflow - Realistic Situation of the Antarctic Circumpolar Current

The next scenario we look at considers a realistic example of the South Atlantic Ocean where mass transport enters and leaves as combination of Scenarios 1 and 2; entering at the southwestern boundary and leaving at both the southeastern and northwestern boundaries, see Figure 10 below.

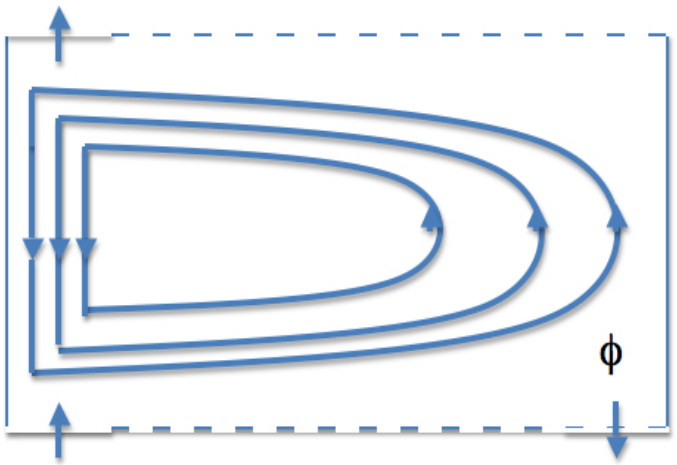


Figure 10: Anticyclonic Gyre Within an Open Basin: Third Scenario.

The example tries to imitate the Malvinas Current and part of the Antarctic Circumpolar Current (ACC). The Malvinas Current is a branch of the ACC that flows northward directly east of South America. The ACC is a current that completes a

whole circuit around the Earth, and is an important ocean current in the Southern Ocean. It encircles the Antarctic continent and whilst it does so it enters the southern basins of the Atlantic, Indian and Pacific Oceans. We are concerned with the ACC entering the Southern Atlantic Ocean.

In terms of mass transport, the ACC is a dominant current in the southern hemisphere. It is estimated that the ACC provides approximately a mean transport of $134 \pm 13\,Sv$ (Whitworth, 1983; Whitworth and Peterson, 1985) through the Drake Passage located below South America. From this approximation, we assume that the inflow in our scenario is approximately $80\,Sv$. We know that much of this easterly flowing current continues through to the Indian Ocean, so we assume that $65\,Sv$ leaves at the southern boundary and only $15\,Sv$ makes it around the basin and leaves at the northern boundary.

Estimating the velocities of the transport entering and leaving the basin is done in a similar fashion as seen previously.

We find that the inflow has velocity $v_3^1 = 1.6\,ms^{-1}$, the outflow at the southern boundary has velocity $v_3^2 = -1.3\,ms^{-1}$ and the outflow at the northern boundary has velocity $v_3^3 = 0.3ms^{-1}$. We have assumed that the depth, $h = 500\,m$ at both north and south boundaries and that the length scale of inflow and outflows are all given by $L_3 = 100\,km$.

We now estimate the terms in the momentum equations using the information above.

### 5.3.1 Zonal Momentum Equation

The first advection term is once again zero due to no normal flow at the boundaries at $x = 0$ and $x = L$. This continues to hold because the east and west boundaries remain closed. Hence

$$\iint_{\phi} (hu^2)_x \, dx \, dy = 0.$$

The second advection term gives us a contribution. We have found from above the velocities in the meridional direction. We assume that these velocities also have a zonal component of $u_3^1 = 0.01\,ms^{-1}$ for the inflow, $u_3^2 = 0.01\,ms^{-1}$ for the southern outflow and $u_3^3 = -0.01\,ms^{-1}$ for the northern outflow. Taking these values allows a contribution for this term, else if they were set to zero, this term would also be zero. We find that

$$\iint_{\phi} (huv)_y \, dx \, dy = \int huv \Big|_{y=0}^{y=M} \, dx =$$

$$\int hu_3^3 v_3^3\,dx - \left(\int hu_3^1 v_3^1\,dx + \int hu_3^2 v_3^2\,dx\right) \approx -3\times 10^5\ m^4 s^{-2}.$$

The next term we approximate is the Coriolis term. We know that of the $80\,Sv$ that enters the basin, $65\,Sv$ leave at the southern boundary. This term tells us the effect of the Coriolis force on the mass transport that travels northward. We have assumed that $15\,Sv$ of the $80\,Sv$ travels northward, then around the gyre to where it exits at the northwestern boundary. We take the approximations of velocity and length scale for the mass transport that leaves and find that

$$\iint_\phi fhv\,dx\,dy \approx fHV_3^3 L_3 M = -3\times 10^9\ m^4 s^{-2}.$$

The frictional term in this scenario is given by

$$\iint_\phi -A\nabla\cdot(h\nabla u)\,dx\,dy \approx 2\times 10^5\ m^4 s^{-2}.$$

Approximating the pressure term in order to conserve the momentum balance, we find that

$$\iint_\phi \tfrac{1}{2}g'(h^2)_x\,dx\,dy \approx -3\times 10^9\ m^4 s^{-2}.$$

We find that as we suggested, the results from this momentum balance is different to the previous scenario. We now have a dominant Coriolis term which is due to the deflecting current that flows out at the northern boundary. The Coriolis term balances with the pressure term, creating a geostrophic flow.

### 5.3.2 Meridional Momentum Equation

We now move onto the meridional momentum equation.

The first advection term in this equation is zero due to the boundary conditions, i.e.

$$\iint_\phi (huv)_x\,dx\,dy = 0.$$

The second advection which is non-zero is given by

$$\iint_\phi (hv^2)_y\,dx\,dy = \int hv^2\Big|_{y=0}^{y=M}\,dx$$

$$= \int h(v_3^3)^2\,dx - \left(\int h(v_3^1)^2\,dx + \int h(v_3^2)^2\,dx\right) \approx -5\times 10^8\ m^4 s^{-2}.$$

We know the Coriolis effect increases with increasing latitude, however, we must remember that in the Southern Hemisphere that this is of a negative sign. The Coriolis force differs from the northern boundary to the southern boundary. We must also recall that the velocity of the mass transport has a sign change halfway in the basin.

We will estimate the Coriolis term for the mass transport flowing westwards at the northern boundary and also for the transport flowing eastwards at the southern boundary. As seen previously we split the basin into two halves. We must use continuity to find the velocities of the two transports as this time they are different as the majority of it leaves at the southeastern boundary.

For the southern half of the basin, we take a small section of the basin and use continuity to give us

$$\begin{aligned}
&\int_0^{M/2}\int_0^{L_3}(hu)_x\,dx\,dy + \int_0^{M/2}\int_0^{L_3}(hv)_y\,dx\,dy = 0\\
\implies &-\int_0^{M/2}(hu)_{x=L_3}\,dy + \int_0^{L_3}(hv)_{y=0}\,dx = 0\\
\implies &\int_0^{M/2}(hu)_{x=L_3}\,dy = \int_0^{L_3}(hv)_{y=0}\,dx.
\end{aligned}$$

Approximating the values in the integrals and by calling the velocity flowing eastwards $u_3^4$ gives us

$$\begin{aligned}
&HU_3^4\tfrac{M}{2} \approx HV_3^1L_3\\
\implies &U_3^4 \approx 0.16\,ms^{-1}.
\end{aligned}$$

Similarly, the westward flowing transport gives us a velocity of

$$U_3^5 \approx -0.03\,ms^{-1}.$$

Note that we have continued the use of the convention of Scaling Analysis, where $h \approx H$, $u_3^4 \approx U_3^4$ and so on.

We can now approximate the Coriolis term as

$$\begin{aligned}
\iint_\phi f hu\,dx\,dy &= \int_0^{M/2}\int_0^{L}(f_0+\beta y)hu\,dx\,dy + \int_{M/2}^{M}\int_0^{L}(f_0+\beta y)hu\,dx\,dy\\
&= \int_0^{M/2}\int_0^{L} f_0 hu\,dx\,dy + \int_{M/2}^{M}\int_0^{L} f_0 hu\,dx\,dy + \int[\beta\tfrac{y^2}{2}hu]_0^{M/2}\,dx + \int[\beta\tfrac{y^2}{2}hu]_{M/2}^{M}\,dx\\
&\approx f_0HU_3^4L\tfrac{M}{2} + f_0HU_3^5L\tfrac{M}{2} + \beta\tfrac{M^2}{8}HU_3^4L + \beta\tfrac{3M^2}{8}HU_3^5L\\
&\approx -6.3\times10^{10}\,m^4s^{-2}.
\end{aligned}$$

Adding the gyre's contribution to the Coriolis term, gives us a total of -6.4 $\times$ $10^{10}\, m^4 s^{-2}$.

The friction term is given by

$$\iint_{\phi} -A\nabla \cdot (h\nabla v)\, dx\, dy \approx -3 \times 10^5\ m^4 s^{-2}.$$

The pressure term is to be found by conservation of momentum. So we find it has to balance the momentum equation by matching the order of magnitude of the Coriolis term. Hence

$$\iint_{\phi} \tfrac{1}{2} g'(h^2)_y\, dx\, dy \approx 6.4 \times 10^{10}\ m^4 s^{-2}.$$

In this direction also, we have a geostrophic balance. The Coriolis term dominates this balance along with the pressure term. The geostrophy concept has shown to be true in both momentum equations here. We used a realistic example of a flow into the South Atlantic, where some of the mass transport is diverted and flows out the from the northern boundary of the basin and we find that this flow is governed by geostrophic balance. The increased eastward flow is the reason for the pressure gradient being much larger in comparison to the previous scenario.

## 5.4 Scenario 4: Eastern Inflow and Eastern Outflow - Realistic Situation of the Agulhas Current

The forth scenario we look at is concerned with the Agulhas current and retroflection within the South Atlantic Ocean. The Agulhas current is a western boundary current which flows southwards, down the southeastern coast of Africa. The northern part of the current is generally quite stable and the southern part is where it meanders in the South Atlantic Ocean. This meandering, at about $37^{\circ}S$, results in eddies and plumes that flow southwestward in the South Atlantic. (De Ruijter et al., 1999).

It is estimated that the Agulhas current carries a mass transport of at least $65\, Sv$. The majority of the current itself is derived from the South Indian Ocean Subgyre in the form of mesoscale rings. These come through the East Madagascar Current. Additional transport contributions come from the east of the Mozambique Channel, where it is estimated at about $5 - 21\, Sv$.

The current itself that retroflects carries much of its mass back with it into the Indian Ocean. This is the Agulhas Return Current. Here at the Agulhas Return Current is where the ring-shedding process begins. Preceding the ring-shedding is

a Natal Pulse event, where the northern part of the current has intermittent solitary meanders. These propagate downstream and occur at around 6 times per year (Lutjeharms and Roberts, 1988; Lutjeharms et al., 2003). If these meanders reach the retroflection, we expect that a ring shedding event will proceed (van Leeuwen et al., 2000).

In this scenario we will examine the existence of the Agulhas Current in the South Atlantic Ocean and look at the momentum balances. We will for now assume that all of the mass transport that enters the South Atlantic Ocean, retroflects back into the Indian Ocean. So we have an inflow of $65\,Sv$ and also an outflow of $65\,Sv$. These will occur on the eastern boundary of our basin (Figure 11).

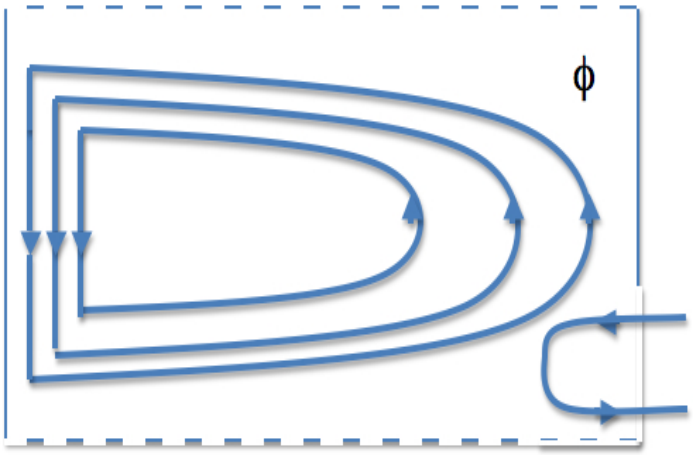


Figure 11: Anticyclonic Gyre Within an Open Basin: Forth Scenario.

### 5.4.1 Zonal Momentum Equation

We begin with the zonal momentum equation. In order to calculate the terms in the equation, we find an approximation for the velocity of the mass transport flowing into the basin. Note that this will be equal and opposite for the transport leaving the basin. So we have that

$$\int hu_4\,dy = 65\times10^6\,m^3s^{-1} \implies HU_4M_4 = 65\times10^6 \implies u_4 \approx 1.3\,ms^{-1}.$$

The above uses a current with width, $M_4 = 100$ km with velocity $u_4 = -1.3\,ms^{-1}$. We have also assumed that the depth remains the same at the eastern boundary of basin, i.e. $h = 500\,m$.

We find that the first advection term now gives us a contribution, this is of order of magnitude given by

$$\iint_{\phi} (hu^2)_x \, dx \, dy = 1.7 \times 10^8 \; m^4 s^{-2}.$$

The second advection term is zero in this case. There is no advection occurring on the north or south boundaries, so

$$\iint_{\phi} (huv)_y \, dx \, dy = 0.$$

As we can see from Figure 11, there must be a Coriolis effect on the mass transport that is flowing southwards on the so called meander, where the current retroflects. The Coriolis term in this equation is approximated by the following

$$\iint_{\phi} fhv \, dx \, dy \approx fHV_4L_4M_5,$$

where $L_4$ is the zonal length scale of the current from where it begins to flow in on the eastern boundary, to where it diverts southwards and $M_5$ is the meridional length scale of the area where the current is acting on. These length scales can be seen in Figure 12. We take $L_4 = 500\,km$ and $M_5 = 400\,km$.

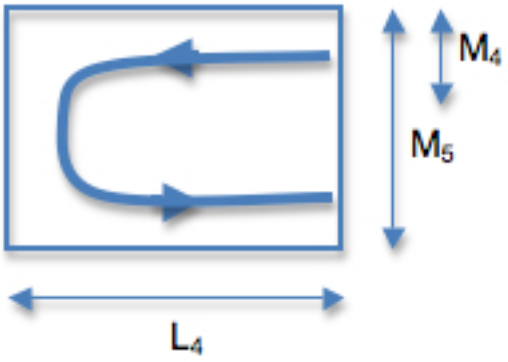


Figure 12: Length scales of Agulhas Current and retroflection area

In order to complete the approximation, we need a value to take for $v_4 \approx V_4$.

Using mass continuity as seen earlier, we have $HU_4M_4 \approx HV_4L_4$.

This now means we can find an approximation to the Coriolis term, by substitution we get

$$\iint_{\phi} fhv\,dx\,dy \approx fHV_4L_4M_5 \approx fHU_4M_4M_5 = 2.6 \times 10^9\, m^4 s^{-2}.$$

Note, the sign is positive due to $f$ being negative and the direction of the $u_4$ being westwards and $v_4$ being southwards respectively means that the velocities are also negative.

The friction term for this scenario is

$$\iint_{\phi} -A\nabla \cdot (h\nabla u)\,dx\,dy \approx 6.5 \times 10^5\ m^4 s^{-2}$$

We find again that the balance so far cannot be true unless the pressure term has its contribution. The pressure term should balance with the advection and Coriolis terms which gives us

$$\iint_{\phi} \tfrac{1}{2} g'(h^2)_x\,dx\,dy \approx 2.4 \times 10^9\, m^4 s^{-2}.$$

The results tell us that for the Agulhas Current and Return Current entering the South Atlantic Ocean, the flow is likely to be in geostrophic balance. However, we have a large contribution also from the zonal advection term in this case. We understand that this is due to the Agulhas Current entering and leaving the basin. Although we have no net mass flowing into the basin, we do have this extra momentum.

The Coriolis term overall is negative due to the sign in the zonal momentum equation, which means in terms of a balance that the pressure term and advection term are both positive. We expect the advection term to be positive due to the mass transport leaking into the basin. The positive nature of the pressure term implies that the depth of the active layer is larger at the eastern boundary compared to the western boundary. We believe that this may be caused by the Agulhas Current forcing the water beneath it down.

We must be careful with the analysis in this situation because, although we expect a geostrophic balance with the flow, we can be unsure about the advection term being as strong as we have found. We have previously used approximations that come mainly from current meter measurement data, but also hydrographic measurements and satellite altimetry which provide us with current estimates. De Ruijter et al. (1999) provides us with the estimate we have used here. Having an uncertainty here makes it difficult to say whether this flow here is in geostrophic balance or not. We can see the pressure term and Coriolis term are the largest terms in the balance so suggest we have geostrophy here.

### 5.4.2 Meridional Momentum Equation

Now we we look at the meridional momentum equation. The first advection term is zero. Earlier we saw that we can find a contribution to a term similar to this one by having the a meridional velocity effect the inflow and outflow. Here, we assume that this is not the case and that there is no meridional component effecting the direction of the inflow and outflow, hence this advection term is zero.

$$\iint_{\phi} (huv)_x \, dx \, dy = 0.$$

Furthermore, we may notice that even with a small southward velocity component of the inflow and outflow, the term also vanishes as the zonal flows are both equal but opposite.

The second advection term is concerned with advection occurring on the north and south boundaries. We have assumed in this scenario that nothing flows in or out on the boundaries so this term is also zero.

$$\iint_{\phi} (hv^2)_y \, dx \, dy = 0.$$

We now move onto the Coriolis term. At a first glance we notice that the inflow is equal and opposite to the outflow. This means that when we use the Beta approximation for the Coriolis parameter, $f$, the term involving the constant $f_0$ is zero. We saw this with the gyre in the closed basin. So what remains is

$$\iint_{\phi} fhu \, dx \, dy = \iint (f_0 + \beta y) hu \, dx \, dy = \iint \beta y hu \, dx \, dy$$

$$= \int \beta \tfrac{y^2}{2} hu \big|_{y=0}^{y=M_5/2} dx - \int \beta \tfrac{y^2}{2} hu \big|_{y=M_5/2}^{y=M_5} dx \approx -\beta H U_4 \tfrac{(M_5)^2}{4} \approx -2.6 \times 10^8 \; m^4 s^{-2}.$$

If we add the gyres contribution to this term we have a total of $-7.6 \times 10^8 \, m^4 s^{-2}$.

The friction term for this current is given by

$$\iint_{\phi} -A \nabla \cdot (h \nabla v) \, dx \, dy \approx 1.625 \times 10^4 \, m^4 s^{-2}.$$

We know the pressure term must contribute here to close the balance, we find that

$$\iint_{\phi} \tfrac{1}{2} g' (h^2)_x \, dx \, dy \approx 7.6 \times 10^8 \, m^4 s^{-2}.$$

We find here that the Coriolis term is balanced by the pressure term in order to conserve momentum. We notice also that there is no advection contribution to this

balance, which is what we expect in this direction. A regular pattern we are finding is that the flow is generally dominated by the Coriolis and pressure terms. With large-scale geostrophic flows, we expect that this is the situation.

We must note that here the pressure gradient term may be zero. We could have a balance between the Coriolis and advection terms if the uncertainties in the advection suggest it should be larger. This would mean the flow is not geostrophic. Bearing this mind, we understand that Agulhas rings are shed due to the retroflection of the Agulhas Current, so we are more interested in the situation that follows.

## 5.5 Scenario 5: The Agulhas Current with Additional Northern Outflow

The fifth scenario we look at is still focused on the Agulhas Current entering the South Atlantic Ocean and the Agulhas Return Current leaving the basin. In the previous scenario, we looked at the case where the mass transport entering the basin, all leaves with the Agulhas Return Current at the area of retroflection. However, in this scenario we look at the momentum balances concerned with the same current entering and leaving the basin but this time, some mass transport travels northwestwards through the basin and leaves at the northern boundary. See Figure 13.

Instead of having the estimated $65\,Sv$ entering the basin as we saw previously, we now have $80\,Sv$ as the inflow from the Agulhas Current. Of this, $65\,Sv$ will be part of the Agulhas Return Current and the other $15\,Sv$ is what leaves at the northern boundary.

The extra $15\,Sv$ must flow around the South Atlantic gyre with the flow until it reaches the western boundary, where it flows out northwards into the North Atlantic Ocean. The outflow here will be done so over a length scale of $L_5 = 100\,km$, as we have seen in the previous scenarios that have a similar outflow to this one.

### 5.5.1 Zonal Momentum Equation

Starting with the zonal momentum equations, the terms are approximated in the same manner. The first advection term with this setup becomes

$$\iint_{\phi} (hu^2)_x \, dx \, dy \approx 2.1 \times 10^8 \; m^4 s^{-2}.$$

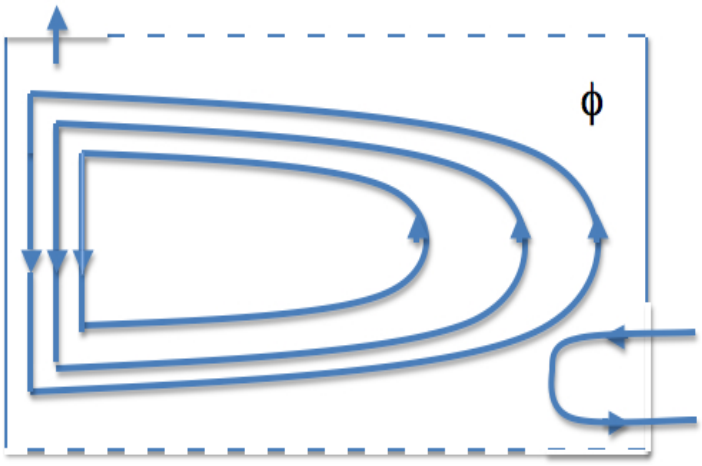


Figure 13: Anticyclonic Gyre Within an Open Basin: Fifth Scenario

The second advection term is zero if the outflow is completely northward. However, it can be non-zero in this scenario. We will assume that a zonal velocity of $u = -0.01\, ms^{-1}$ affects this outflow in order to get a contribution, we find that

$$\iint_{\phi} (huv)_y \, dx \, dy \approx -1.5 \times 10^5 \; m^4 s^{-2}.$$

We estimate the Coriolis term using the methods used in Scenarios 2 and 4. In scenario 2, we used a value of $f$ at mid-basin and approximated the Coriolis term for the mass transport flowing northwards near the eastern boundary and in Scenario 4, we approximated it in the smaller area where the Agulhas Current was flowing. Combining the two methods we get an approximation to this term given by

$$\iint_{\phi} fhv \, dx \, dy \approx fHV_5L_5(M - M_5) + fHU_5M_4M_5 \approx 8 \times 10^8 \; m^4 s^{-2}.$$

The friction term in the zonal direction is

$$\iint_{\phi} -A\nabla \cdot (h\nabla u) \, dx \, dy \approx -5.8 \times 10^5 \; m^4 s^{-2}.$$

And finally the pressure term here must act in order to balance this equation. We see the advection and Coriolis terms are dominant here, thus we find that the pressure term is given by

$$\iint_{\phi} \tfrac{1}{2} g' (h^2)_x \, dx \, dy \approx 5.9 \times 10^8 \; m^4 s^{-2}.$$

We find here something similar to what we found in the previous scenario. The advection due to the Agulhas Current entering the basin is a term which is included in the momentum balance as well as the pressure and Coriolis terms.

As mentioned earlier, we suggested that the Agulhas Current's estimation may have uncertainties involved with it. Here we have taken a larger value for the inflow than used previously so we expect that the advection term will be larger also due to extra momentum in the basin. A larger estimate for the inflow has been used to account for mass transport that flows out at the northern end of the basin and still retain a reasonable value for the Agulhas Return Current.

So here we find a balance between three terms, which include an advection term, the pressure term and the Coriolis term. This balance provides us with a different relationship to what we found when we had geostrophic balance. This balance has no theoretical explanation behind it and the occurrence of the extra advection term implies we do not have a geostrophic flow.

Here we can also expect that the balance can be between the Coriolis and advection terms, this is a possible momentum balance. Although the local balance within the basin can be mainly geostrophic, the large-scale integrated balance can be different.

The extra momentum related to the advection here could be related to the eddy formation and Agulhas rings. The existence of this term has appeared in both the Agulhas Leakage scenarios in the zonal direction. The Agulhas rings may be the reason for why this extra momentum is appearing in the advection term.

### 5.5.2 Meridional Momentum Equation

Next we examine the meridional momentum equation. Firstly, the first advection term in this equation depends on the direction of the inflow and outflow of the Agulhas Current. Previously in the zonal equation, we stated that we would use no component of a velocity $v$ affecting the this current into and out of the basin. If so, then this term is zero. If there was a southward component of, say $v = -0.01\, ms^{-1}$, then the contribution is

$$\iint_{\phi} (huv)_x \, dx \, dy = 1.5 \times 10^5 \; m^4 s^{-2}.$$

The second term is advection on the north and south boundaries. We have advection occurring on the northern boundary and this is given by

$$\iint_{\phi} (hv^2)_y \, dx \, dy = 4.5 \times 10^6 \; m^4 s^{-2}.$$

The Coriolis term in this equation is split into two different approximations. One uses the same method as seen in the previous scenario and the other approximates the Coriolis term on the mass transport flowing westwards in the northern half of the basin, similar to the approximation is Scenario 3.

Firstly, the contribution from the Agulhas Current inflow and Agulhas Return Current outflow, is given by

$$\iint_{\phi} fhu\,dx\,dy = \iint (f_0 + \beta y)hu\,dx\,dy$$

$$= \iint_0^{M_5/2} f_0 hu\,dx\,dy + \int \beta\tfrac{y^2}{2}hu|_{y=0}^{y=M_5/2}\,dx + \iint_{M_5/2}^{M_5} f_0 hu\,dx\,dy + \int \beta\tfrac{y^2}{2}hu|_{y=M_5/2}^{y=M_5}\,dx\,m^4s^{-2}$$

$$\approx 4\times10^9 + 1.3\times10^8 - 3.25\times10^9 - 4.8\times10^8 = 4\times10^8\,m^4s^{-2}.$$

Secondly, is the approximation for the westward flow in the northern half of basin. Using mass continuity, we know that $15Sv$ leaves the basin at the northern boundary, so the westward flow of the transport has velocity $u_5 = -0.03\,ms^{-1}$ over the distance of half the basin, i.e. $1000\,km$. We find the contribution given by this flow is

$$\iint (f_0 + \beta y)hu\,dx\,dy \approx f_0 H U_5 L\tfrac{M}{2} + \beta\tfrac{3(M)^2}{8}HU_5L \approx 5.3\times10^9\,m^4s^{-2}.$$

The total contribution of the Agulhas Current and westward flow in the basin is $5.7\times10^9\,m^4s^{-2}$ We must add the contribution from the gyre to this and we have the full approximation of the Coriolis term which is given by

$$\iint fhu\,dx\,dy \approx 5.2\times10^9\,m^4s^{-2}.$$

The friction term for this scenario is

$$\iint_{\phi} -A\nabla\cdot(h\nabla v)\,dx\,dy = 2.5\times10^3\ m^4s^{-2}.$$

The pressure term here must act to balance this equation and is given by

$$\iint_{\phi} \tfrac{1}{2}g'(h^2)_y\,dx\,dy \approx -5.2\times10^9\ m^4s^{-2}.$$

In the zonal momentum equation, we found a balance that involved an advection term along with the Coriolis and pressure term. However, in this direction, we are back to having the latter two terms being dominant.

We find that the pressure term in this direction is negative for the momentum equation to balance. Physically this means that the depth of water in the active layer is now shallower at the northern boundary than at the southern boundary.

In terms of a geostrophic flow, we know that the Coriolis term acts towards the left of the flow and the pressure gradient is towards the right. Here, we discover the

opposite occurring and find an interesting result.

We find that although we have a net westward flow present, the eastward flowing current is situated further south and gives rise to a stronger Coriolis force. The result this leads to is a net northward Coriolis force. We have in this case local geostrophy present but the large-scale balance is different due the variation of the Coriolis parameter with latitude.

The inclusion of the advection term in the zonal momentum balance has appeared twice and we may still expect that this is something to be aware in consideration of the large-scale momentum balances on the South Atlantic Ocean.

# 6 The Agulhas Influence on the Overturning Circulation. What is actually going on?

From examining the different scenarios of mass transport into and out of the basin in Section 5, we are now in a position to put them all together and configure the realistic situation. We will again use the momentum equations to find out how the Agulhas leakage is influencing the overturning circulation. We know where the water enters and leaves the basin, we also have estimates for the amount of water flowing in and out, but we are unsure of what the mass transport is actually doing within the basin. We aim to look at what the momentum balances can tell us about the South Atlantic Ocean.

The Agulhas leakage is where large oceanic rings are shed from the retroflecting Agulhas Current. It is an interocean exchange between the Atlantic and Indian Oceans (W Weijer, 2002). The Agulhas leakage has an important influence on the Overturning Circulation, providing heat and salt into the Atlantic Ocean. A change in the Agulhas leakage could lead to major changes on the Overturning Circulation. Increasing freshwater fluxes can cause the Ocean's Conveyor to completely shutdown (W. S. Broecker, 1991) and may only be overcome by increased salinity in the Atlantic Ocean. These changes can cause abrupt climate changes and it is important to realise the ocean plays a dominant role in this along with the atmosphere.

There are two possible situations in which we think the Agulhas leakage could have an impact on the circulation. The first is where part of the Agulhas current that retroflects back into the Indian Ocean, flows northwards around the gyre, then westwards towards the western boundary and then northwards again out the basin. In addition to this is, we have the ACC that enters at the southwest and flows eastwards out into Indian Ocean. We assume that the ACC does not contribute to the transport leaving the basin at the northern boundary. A diagram of this situation can be see in Figure 14.

The second situation is similar to the above except that the Agulhas Current that retroflects provides no diverted mass transport. In other words, all the mass transport that enters on the eastern boundary, leaves on the same boundary. The difference is that the ACC provides the mass transport that leaves the basin at the northern boundary, however, most of this current also leaves the basin where the Agulhas Return Current leaves. This situation is depicted in Figure 15.

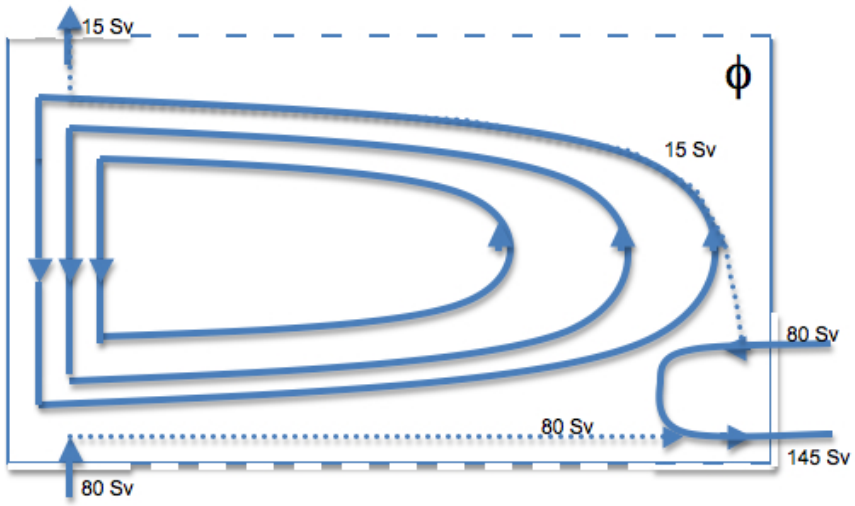


Figure 14: Configuration suggesting the northern outflow is from the Agulhas leakage.

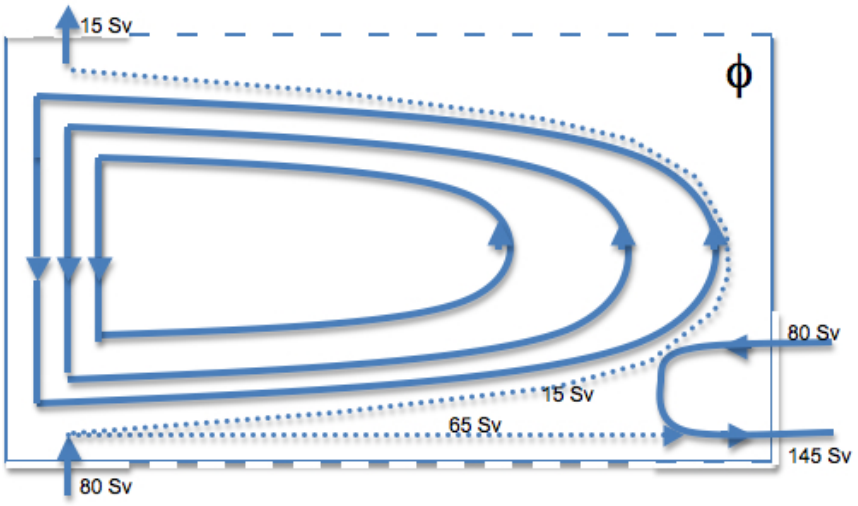


Figure 15: Configuration suggesting the northern outflow is from the ACC.

## 6.1 Momentum Balances for the Agulhas Leakage Providing the Outflow at the Northern Boundary

As seen in §5, we return to the momentum equations and try to figure out the momentum balances for the situation where the Agulhas leakage provides the outflow at the northern boundary of our basin.

We begin with the advection terms in the zonal momentum equation. The advection we have here is on the eastern boundary and from the Agulhas Current, Return Current and the easterly flowing ACC. We find that

$$\iint_{\phi} (hu^2)_x \, dx \, dy \approx 5.5 \times 10^8 \; m^4 s^{-2}.$$

The second advection term is zero, since we take the entering ACC and outflow current as completely meridional so it has no $u$ velocity component, i.e.

$$\iint_{\phi} (huv)_y \, dx \, dy = 0.$$

The Coriolis term in this direction depends on the transport flowing northward from the Agulhas Current and the southward flowing Agulhas Current, so we have

$$\iint_{\phi} fhv \, dx \, dy \approx fHV_5L_5(M - M_5) + fHU_5M_4M_5 \approx 8 \times 10^8 \; m^4 s^{-2}.$$

Note that this is the same as Scenario 5, the additional ACC does not contribute to this term. We have also made use of mass continuity in the latter approximation of the Coriolis term.

The friction term in the zonal momentum equation is approximated as

$$\iint_{\phi} -A\nabla \cdot (h\nabla u) \, dx \, dy \approx 4.8 \times 10^6 \, m^4 s^{-2}.$$

We find that we have large contributions from the advection and Coriolis terms however, the pressure terms remains to be approximated. In order to balance this equation correctly, we find that the pressure term has to be

$$\iint_{\phi} \tfrac{1}{2} g' (h^2)_x \, dx \, dy \approx 2.5 \times 10^8 \; m^4 s^{-2}.$$

Moving onto the meridional momentum equation, we find the approximations for the terms are as follows.

The first advection term is

$$\iint_{\phi} (huv)_x \, dx \, dy = 0.$$

using the reasoning that the inflow and outflow from the Agulhas Current on the eastern boundary are completely zonal.

The second term, the advection on the north and south boundaries is given by

$$\iint_{\phi} (hv^2)_y \, dx \, dy = 1.2 \times 10^8 \; m^4 s^{-2}.$$

The Coriolis term in this equation must be split into three different approximations, all of which we have seen previously. These take into account the Coriolis force acting on the water flowing eastwards, westwards and the water that is apart of the Agulhas Current and retroflection.

The contribution from the Agulhas Current inflow and Agulhas Return Current outflow is the same as that calculated in the previous scenario. This is given by

$$\iint\limits_{\phi} fhu\,dx\,dy \;=\; \iint (f_0+\beta y)hu\,dx\,dy$$

$$= \iint_0^{M_5/2} f_0 hu\,dx\,dy + \int \beta\tfrac{y^2}{2}hu\big|_{y=0}^{y=M_5/2}\,dx + \iint_{M_5/2}^{M_5} f_0 hu\,dx\,dy + \int \beta\tfrac{y^2}{2}hu\big|_{y=M_5/2}^{y=M_5}\,dx$$

$$\approx 4\times10^9 + 1.3\times10^8 - 3.25\times10^9 - 4.8\times10^8 = 4\times10^8\, m^4s^{-2}.$$

The westward flow in the northern half of basin is also the same as the previous scenario. The contribution given by this flow is

$$\iint (f_0+\beta y)hu\,dx\,dy \approx 5.3\times10^9\, m^4s^{-2}.$$

The final contribution is from the water flowing eastwards in the southern half of the basin. This approximation, using mass continuity, is

$$\iint fhu\,dx\,dy \approx fHULM_4 \approx fHVLL_4 \approx -4\times10^{10}\, m^4s^{-2}.$$

The total contribution is $-3.4\times10^{10}\, m^4s^{-2}$. Moreover, we must add the contribution from the gyre to this and we have the full approximation of the Coriolis term which is

$$\iint fhu\,dx\,dy \approx -3.5\times10^{10}\, m^4s^{-2}.$$

The friction term is

$$\iint\limits_{\phi} -A\nabla\cdot(h\nabla v)\,dx\,dy = 7.1\times10^5\; m^4s^{-2}.$$

And finally, the pressure term. We already know that this term should act to balance to the momentum equation and we find that the pressure term in this scenario is given by

$$\iint\limits_{\phi} \tfrac{1}{2}g'(h^2)_y\,dx\,dy \approx 3.5\times10^{10}\; m^4s^{-2}.$$

Now we look at the second situation, where the Agulhas Current does not provide the transport that leaves at the northern basin. It is provided by the ACC.

We begin with the advection terms, they are the advection on the boundaries and since this is the same as the previous case, they are no different. They are

$$\iint_{\phi} (hu^2)_x \, dx \, dy \approx 5.5 \times 10^8 \ m^4 s^{-2}$$

and

$$\iint_{\phi} (huv)_y \, dx \, dy = 0.$$

The Coriolis term however, is different, it depends on the transport flowing northward from the ACC and the southward flowing Agulhas Current. We have

$$\iint_{\phi} fhv \, dx \, dy \approx fHV_{north} L_5 (M - M_5) + fHU_{80sv} M_4 M_5 \approx 2 \times 10^8 \ m^4 s^{-2}.$$

The friction term is given by

$$\iint_{\phi} -A\nabla \cdot (h\nabla u) \, dx \, dy \approx 4.8 \times 10^6 m^4 s^{-2}.$$

In order to balance the equation, the pressure term now turns out to be

$$\iint_{\phi} \tfrac{1}{2} g' (h^2)_x \, dx \, dy \approx -3.5 \times 10^8 \ m^4 s^{-2}.$$

We also find the approximations for the meridional momentum equation. The advection terms are the same as the previous situation where

$$\iint_{\phi} (huv)_x \, dx \, dy = 0$$

and

$$\iint_{\phi} (hv^2)_y \, dx \, dy = 1.2 \times 10^8 \ m^4 s^{-2}.$$

The Coriolis term is split into three cases, firstly looking at the transport of 15 $Sv$ that flows eastwards then westwards, then for the 65 $Sv$ eastward transport that flows out with the Agulhas Return Current and the third is for the Agulhas Current.

We have for the 15 $Sv$ transport

$$\iint_{\phi} fhu \, dx \, dy = \iint \beta y hu \, dx \, dy \approx -\beta \tfrac{M^2}{4} HUL_4 = -3 \times 10^8.$$

Noting that the transport in the southern half is equal and opposite to the transport in northern half, so the $\iint f_0 hu \, dx \, dy$ term cancels.

Secondly for the transport of 65 $Sv$ flowing eastwards, we have

$$\iint fhu\,dx\,dy \approx fHULM_4 \approx -3.3 \times 10^{10}\, m^4 s^{-2}.$$

Finally, for the Agulhas Current we have

$$\iint\limits_{\phi} fhu\,dx\,dy = \iint \beta y hu\,dx\,dy = \int \beta \tfrac{y^2}{2} hu|_{y=0}^{y=M_5/2}\,dx + \int \beta \tfrac{y^2}{2} hu|_{y=M_5/2}^{y=M_5}\,dx$$

$$\approx 1.6 \times 10^8 - 4.8 \times 10^8\, m^4 s^{-2},$$

since we know that the amount flowing westwards is equal to the amount flowing eastwards.

The total contribution of the is $3.3 \times 10^{10}\, m^4 s^{-2}$. We must add the contribution from the gyre to this and we have the full approximation of the Coriolis term which is

$$\iint fhu\,dx\,dy \approx -3.4 \times 10^{10}\, m^4 s^{-2}.$$

The friction term is as found previously, given as

$$\iint\limits_{\phi} -A\nabla \cdot (h\nabla v)\,dx\,dy = 7.1 \times 10^5\ m^4 s^{-2}.$$

Finally, the pressure term is found in order to balance the equation and is given by

$$\iint\limits_{\phi} \tfrac{1}{2} g'(h^2)_y\,dx\,dy \approx 3.4 \times 10^{10}\, m^4 s^{-2}.$$

We find that in both scenarios, the advection terms are identical. This is expected to be the case here as we are looking at the large-scale momentum balances and the same mass transport is entering and leaving the basin in both scenarios. The advection terms take account of what is occurring at the boundaries of the basin, and this is where the advecting mass transport take place.

We notice this is also the case with the friction terms because the transport flowing within the basin is the same in both scenarios; it is the diverted transport which differs. The friction term cannot account for this difference.

However, the Coriolis term can distinguish this difference and where it becomes apparent is in the zonal direction. Here, we find a difference between the two scenarios which leads us to differences in the pressure terms. Although there is no notable difference in the Coriolis terms calculated in the meridional direction, it is the zonal Coriolis term which is of most interest to us here.

## 6.2 Does the Agulhas Current Provide the Outflow at the Northern Boundary?

In Section 6.1 we found estimates of the terms in the momentum equations with two different scenarios put out. We are looking to obtain an answer around what is providing an outflow at the northern boundary of the South Atlantic Ocean. We have used scenarios that suggest it is either the Agulhas Current or the ACC.

From the approximations evaluated previously, we find that the momentum balances are highly similar in both cases. The advection terms, pressure terms and friction terms do not change in the two cases and although the two situations are different, the integrated momentum equations do not fully distinguish between the two. The flows at the boundaries and within smaller areas, for example the area in which the Agulhas Current flows into, do not provide major differences to be noticed in the the momentum equations. However, we are concerned with the momentum balances; momentum has to be conserved and therefore, we must look carefully at this.

Starting in the meridional momentum equation, the two cases are almost exactly the same in regards to every term. A difference we notice is the Coriolis term that differs by $2 \times 10^9\, m^4 s^{-2}$. In comparison to the meridional advection term, this is a large amount. The balance we find is a geostrophic balance here, between the Coriolis and pressure terms. Without much else to the balance, we cannot yet say anything about the Agulhas leakage.

Moving onto the zonal momentum equation, we find the balance involves an advection term, the pressure term and the Coriolis term. This time however, the Coriolis term differs by a factor of 4. Where the Agulhas leakage provides the outflow, the term is larger. In terms of a momentum balance, this may be important. Table 3 shows the three dominant terms in both situations.

| | Agulhas leakage | ACC |
|---|---|---|
| Term | Approximation $m^4 s^{-2}$ | Approximation $m^4 s^{-2}$ |
| $\iint (hu^2)_x \, dx\, dy$ | $5.5 \times 10^8$ | $5.5 \times 10^8$ |
| $-\iint fhv \, dx\, dy$ | $-8 \times 10^8$ | $-2 \times 10^8$ |
| $\iint \frac{1}{2} g' (h^2)_x \, dx\, dy$ | $2.5 \times 10^8$ | $-3.5 \times 10^8$ |

Table 3: Comparison of terms in zonal momentum equation, based on which current provides the outflow at the northern boundary.

Table 3 is gives us great insight to what is occurring with both scenarios. We find a comparative difference for the two cases which is based on the depth of the layer

in the zonal direction.

The result we have is that the Agulhas leakage situation has a momentum balance that implies that the height profile at the eastern boundary is greater than the height profile at the western boundary. However, the ACC gives us the opposite result, where the depth is greater at the western boundary than the eastern boundary.

With the Agulhas leakage configuration, the depth profile shows a positive gradient (from east to west). The transport that travels away from the Agulhas leakage may have an effect on this. We suggest that here most action is taking place, in comparison to the western boundary causing a deeper layer at the this boundary. The momentum due to the mass transport at this could be having an impact here.

Whereas the ACC provides the opposite zonal profile. This may suggest that the transport diverted from this current does not flow as close to the eastern boundary as expected. It may either spread out and become a wider current whilst it travels northwards, or it flows northward closer to the centre of the basin. Either idea may be the reason for why the western boundary is deeper than the eastern boundary.

The above gives us some important results that have been found from the large-scale momentum balances. We must note here that the gyre enclosed in the basin has no effect on the zonal Coriolis term and advection terms coming from the momentum equation. We know that the pressure term has to balance with these terms.

Aside from the momentum balance, we must be aware of any discrepancies in the estimated terms. Oceanographic studies have already provided us with a good understanding of the oceans, gyres and currents around the world. The difficulties we are faced with come in many forms, ranging from the interaction with the atmosphere to understanding mean and transient currents.

It is important to recognise that where we have used order of magnitude estimates, we must be aware of the uncertainties involved with them. For instance, in the two scenarios here, we have an understanding of the mass transports leaving the basin. However, we cannot be certain of the estimates used for each current and transport within the basin. Measurements are obtained from hydrographic data, Lagrangian measurements such as the use of tracers and remote measurements such as satellite altimetry. Each form has its uncertainties involved with them. Given that we know uncertainties are present, they do not become invalid. They do provide us with reasonable estimates for large-scale ocean circulations.

We understand that there will be uncertainties involved with flow velocities and length scales used, but it is fair to assume that the order of magnitude approximations are also the most appropriate means for attempting to find the momentum

balances in each of the scenarios used so far.

Returning to the momentum balances, we find that it is difficult to say we have one clear answer. We cannot confirm where the diversion comes, either from the Agulhas leakage or the ACC. This leads us to a situation where measurements are be taken to confirm which configuration we have in the South Atlantic. We find important results from the momentum balances here but leads us to a study that entails depth measurements in which future studies should incorporate. However, with that option unavailable to us, we try to address this problem using the vorticity balances.

# 7 Vorticity Balances on the South Atlantic Ocean

## 7.1 Numerical Model Outputs

We now focus on the numerical model to provide us with visual and numerically calculated terms in the vorticity equation. We begin to look at numerically generated plots to try to aid our understanding of the vorticity balance when the Agulhas leakage is introduced into the basin.

Figures 16 and 17 show the numerical model's output of the South Atlantic Ocean, separated by an island on the eastern boundary that can be amended to provide us with closed and open basins respectively.

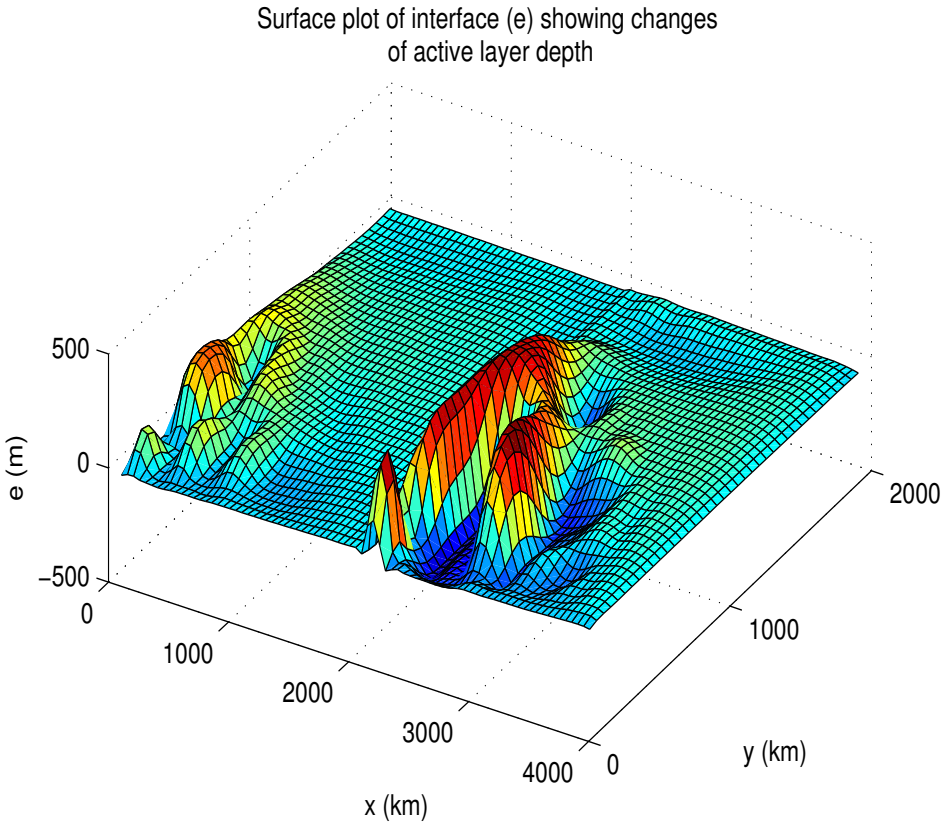


Figure 16: Closed basin: Configuration of wind-driven gyres of the South Atlantic and Indian Ocean basins with an island, full closed, allowing no connection between the two. Interface (e) is given by e = h - 500 m.

The surface wind-stress over the Indian Ocean has twice the strength of that over

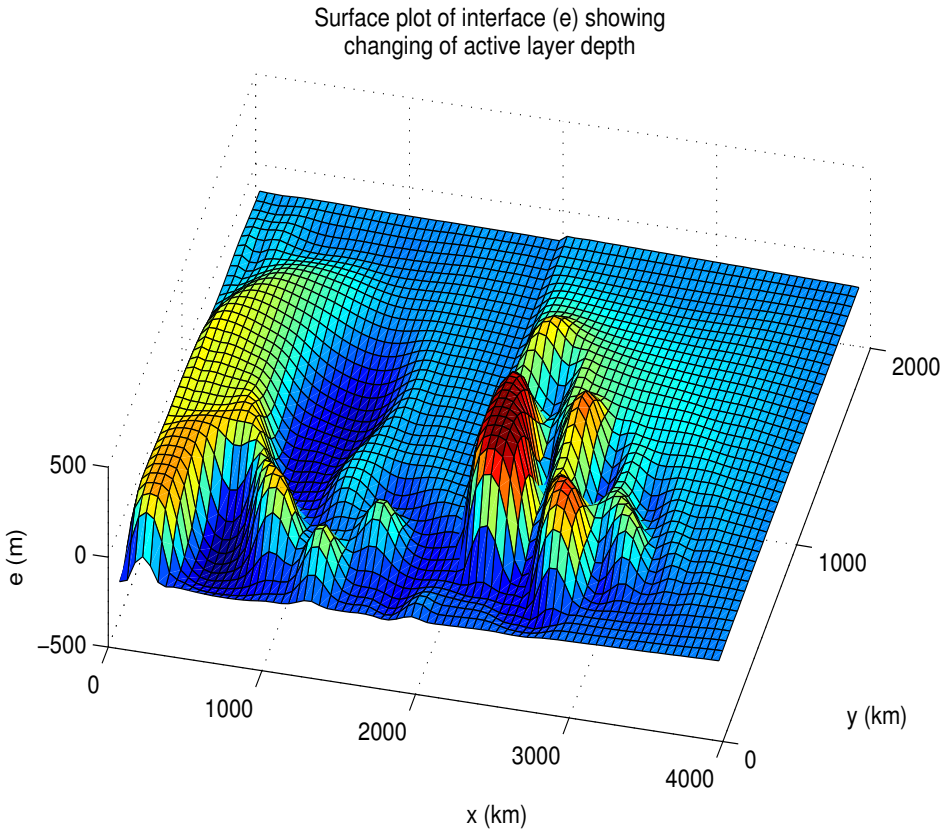


Figure 17: Open basin: Configuration of wind-driven gyres of the South Atlantic and Indian Ocean basins with an island, partly open, allowing a connection between the two. Interface (e) is given by e = h - 500 m.

the South Atlantic in these model outputs here, this is given by $0.2\,Pa$. This value is chosen here to clearly show vorticity within the open basin. The plots have been taken at a model run-time of 1000 days. We notice that in the South Atlantic the action is occurring mostly at the southwest of the basin. We expect that due to the western boundary current, large amounts of friction is produced. Vortices that we can see are produced by instabilities of the western boundary current and due to the separation of this current from the coast in the south of the domain. Friction is due to large gradients in the velocity fields and we see this when the vortices are formed.

We also recognise that this is there are not much taking place in the rest of this basin. We know the currents are smaller elsewhere and is demonstrated in the numerical model. We must pay particular attention to the eastern boundary where the island is closed at the moment as this is where we expect to find an interruption

from rings shed here.

Figure 17 shows an open basin, where the island does not extend all the way down to the southern boundary. This produces an output showing the influence of the Agulhas leakage in the ocean basin. Previously, near the eastern coast of the closed basin, there was not much happening. However, now we notice the shedding of rings into the basin. The friction at the western boundary is still there and acts over a larger area than previously.

The movement of the rings into the basin occur separately suggesting they are shed at different times. After 3 years, we notice at least 3 rings have been shed into the basin. After 3000 days we will have more than 3 rings produced. Their average speed will be approximately $\beta R_d^2$ which is a few $cms^{-1}$. The interaction of the rings in the South Atlantic Ocean is now apparent.

Up until now we have looked thoroughly at the momentum equations, examining them on the closed basin and different situations of an open basin. This lead us to a realistic situation involving the Agulhas leakage and ACC. We have so far found many scenarios that were governed by geostrophic balance and others that were more complicated. These balances included advection terms.

Understanding the Agulhas leakage influence on the South Atlantic by looking at the vorticity equation is to be studied. We previously looked at vorticity in the closed basin and found from this that the diffusivity coefficient should be larger to provide a vorticity balance. However, we noticed it was difficult to approximate the vorticity stretching term since it cancelled due to the geostrophic relationship.

We now wish to look at the vorticity balance of Agulhas leakage but this time by using our numerical model. The model generates two wind-driven gyres being the South Atlantic and Indian Oceans, separated by an island which can be modified to give us a closed basin or an open basin in which the Agulhas leakage can enter the basin; a model of the real world phenomenon. We note that no numerical runs with open boundaries, around the basin itself have been done because these lead to ill-posed numerical problems that are hard to solve.

Furthermore, by numerically calculating the terms in the vorticity equation, we are able to overcome the difficulty in analytically calculating the stretching term and find estimates for all the terms over the basin and see where they are acting within the basin. In regards to estimating the terms, we average them over a given time, which does not start at the initial run of the model as the model has to reach a statistical equilibrium first before this can take place. We know large Agulhas rings are shed from the Agulhas Retroflection and we expect to see what the vorticity balance in light of the numerical model can tell us.

## 7.2 Vorticity Within the Basin

### 7.2.1 Closed Basin Integrated Terms

Using our numerical model we now look at the basin integrated terms in the vorticity equation. We begin with the closed basin, where the island fully encloses the South Atlantic. The terms outputted are the time-averaged terms, for a run of a 1000 days and averaged from 300 days. A run of this length suffices for the closed basin scenario since vorticity from the Agulhas leakage is not going to be apparent here.

The first term is the time dependent term given by

$$(h\zeta)_t = -3\, ms^{-2}.$$

The zonal advection term that we are interested in is

$$(hu\zeta)_x = -19\, ms^{-2}.$$

The stretching term that we stated earlier is difficult to approximate is

$$h(f+\zeta)(u_x + v_y) = -27\, ms^{-2}.$$

The Beta term is

$$\beta h v = 32\, ms^{-2}.$$

The wind-stress term is

$$h\left(\frac{\tau^{(x)}}{h\rho}\right)_y = -393\, ms^{-2}.$$

Finally the friction term is

$$A\left(\zeta_{xx} + \zeta_{yy}\right) = 412\, ms^{-2}.$$

We find that the time dependent term is small as expected; we are running the model to a statistical equilibrium and this term is showing this is true. The zonal advection term within the basin is small also as expect in the closed basin case. We notice that the stretching and Beta term are small and similar in magnitude but have opposite signs; this confirms that they do tend to cancel with each another. We find the dominating terms are the wind-stress and friction terms which act to balance each other and represent the vorticity balance in the closed basin.

Importantly, the vorticity balance we find here in the closed basin from the numerical model agrees with the analytical calculations found earlier for the vorticity equation in Section 4.4. We found that the wind-stress was dominant and the friction term

was the only term able to balance it. Here, the numerically modelled integrated terms give us a confirmation of that result.

The result we are interested in, is the comparison of the vorticity balance with the momentum balance. We found that the pressure gradient and Coriolis terms were dominant in the momentum equation. However, now the vorticity balance is seen to be from the wind input and the friction. This shows us how the different sets of equations emphasise different aspects of the physics for our basin, yet the equations originate from the same basis.

### 7.2.2 Open Basin Integrated Terms

We now look at the basin where the island is open, so it allows the Agulhas leakage to enter the basin. This time, for the ocean to reach a statistical equilibrium we have increased the run-time to 3000 days and taken an average from 1500 days for the time integrated terms.

The time dependent term is

$$(h\zeta)_t = -4\, ms^{-2}.$$

The zonal advection term is

$$(hu\zeta)_x = -74\, ms^{-2}.$$

The stretching term is

$$h(f+\zeta)(u_x + v_y) = -216\, ms^{-2}.$$

The Beta term is

$$\beta h v = -13\, ms^{-2}.$$

The wind-stress term is

$$h\left(\frac{\tau^{(x)}}{h\rho}\right)_y = -333\, ms^{-2}.$$

Lastly, the friction term is

$$A\left(\zeta_{xx} + \zeta_{yy}\right) = 640\, ms^{-2}.$$

We now find a balance which involves the stretching term along with the friction and wind-stress. The stretching contribution is not entirely clear however, it is related to the more ageostrophic character of the flow. The large stretching term is most probably the strong meridional acceleration in the western boundary current due

to the meridional pressure gradient. This is related to the extra mass and vorticity input due to the Agulhas rings, but how exactly is unclear.

The time dependent term is also small and this should be the case as mentioned with the closed basin case. We expect that in both closed and open basins that the Beta term is larger due to the western boundary current however, this seems to be encapsulated by the stretching term.

Again friction and wind-stress are also dominant showing a different side to the ocean physics here in comparison to the geostrophy that we find in the momentum balances. With the momentum balances for the Agulhas leakage we found a large advection term in the momentum balance also. The term shows a reasonable contribution but not as much as we would expect to see. The vorticity input by the boundary is still relatively small in comparison to the real world where we find that the Agulhas rings are as large as the vorticity input by wind. A higher model resolution may capture this but is expensive to implement.

Rather then observed inaccuracies in the ocean magnitudes, we find here that the model may not observe the detail that we might expect. Again, the balance it provides us gives us a good insight to our physical understanding but this can always be improved, especially computationally. Increasing the horizontal resolution requires more computational power and this is a limiting factor here. Nonetheless, the model is adequate and does provide enough detail and explains the vorticity balance we have.

### 7.2.3 Vorticity Fields on the Open Basin

The vorticity equation has different contributions and these individual contributions can be seen as 2-dimensional fields from the model output. We continue to use the 3000 day run and look at the images at this moment in time. These fields can be seen in Figure 18.

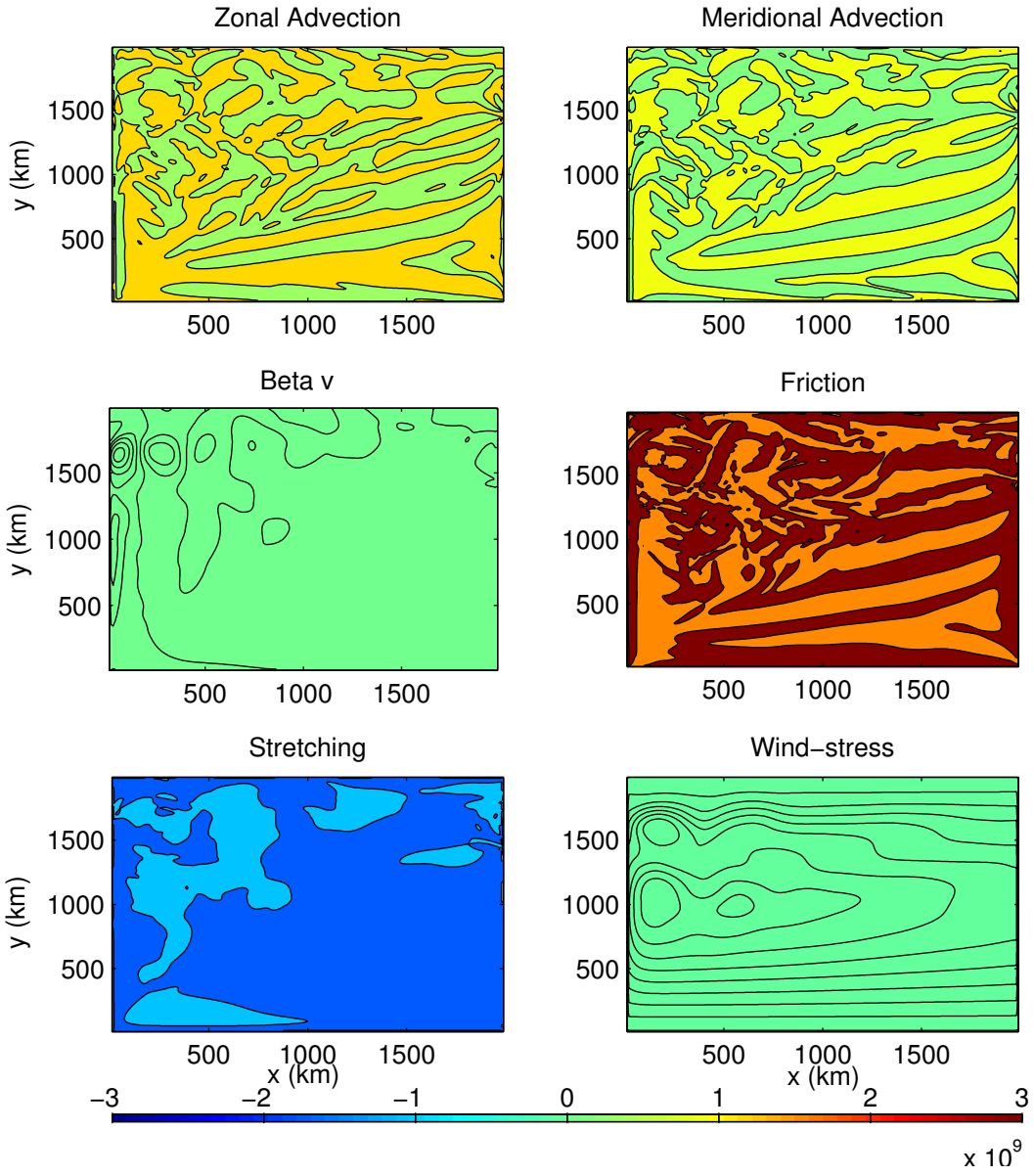


Figure 18: Fields of the terms in the vorticity equation.

The vorticity contributions seen as images in Figure 18 show us the interior features of the basin. Here the model parameters remain the same, we note also that the wind-stress forcing over the Indian Ocean is given by $0.1\,Pa$.

We find that the two advection terms show wave-like features, we see the troughs and crests visible in both situations. However, we find that there is a balance

between the two, they act in a manner such that they tend to cancel with each other. They show vorticity signs in the western boundary and show clearly the input via the Agulhas rings moving into the basin. The eddies moving into the basin can be seen; they are noticed by the smoothed out paths as the eddies move across.

The Beta term also shows signs of a wave-like feature but this is prominent in the western boundary current. The eddies are not picked up too well by this term. The reason for this is to do with the intensification at the western boundary current. Here, we have a strong southward flowing velocity at the western boundary; this term is affected mostly by the strong meridional velocities, it is effectively the sign of the velocity, $v$ and this field shows this well.

The friction term shown is the largest term throughout the basin. Most variation occurs in the south-west area of the basin, where the western boundary current is creating vorticity as it meets the southern boundary. Furthermore, we notice the friction caused by the eddies being introduced into the basin and the movement of them into the basin. We find that the stretching term follows a similar patter except it is occurring mostly at the western boundary and also in the south east domain of the basin where we have newly introduced vorticity. The wind-stress curl is small but is positive throughout, this leads to a large term when integrated over the basin. We notice also this is maximum halfway in the basin.

We are able to see the balance between the advection terms throughout the basin. We also see there is a balance with the stretching and Beta terms with the friction within the western boundary current. The dominating terms of opposite sizes are the friction and the stretching term and confirm the findings in the averaged integrated terms, with exception to the wind-stress.

## 7.3 What does the vorticity balance tell us?

The forefront of our argument here, is that the ACC inflow and outflow to the northern boundary brings in little extra vorticity, whilst the Agulhas leakage configuration does. The numerical experiments show that the extra vorticity from the Agulhas leakage does have a large influence on the vorticity balance, which is expected to be even larger in the real world. We mentioned earlier that the anticyclonic vorticity entering the basin has been estimated to be as large as that due to the wind input which we have seen is a dominant term.

The addition of extra vorticity makes the fluid motion more vigorous and ageostrophic. We noticed that we have a strong stretching term which shows this. The large

stretching term found has a significant impact on the thermocline motions and hence an impact on the Thermohaline Circulation.

The vorticity impacts of the Agulhas rings are seen in the numerical plot of the basin as well as within the vorticity fields. The fields in Figure 18 show that at the eastern boundary the eddy terms are visible in all the terms.

The momentum balances give us an insight to there being an additional advection term within the basin when the Agulhas leakage is present and with our numerical model we notice that the extra vorticity has an impact on the vorticity balance. This vorticity balance tells us that there is an impact from the Agulhas leakage on the large-scale ocean circulation.

# 8 Impacts of the Agulhas Leakage

The vorticity balances on the open basin show that friction, wind-stress and stretching terms are dominant. The friction and stretching terms are large and we suggest that rings are induced by the significant amount of anticyclonic vorticity within the basin.

The vorticity input from the Agulhas leakage was seen in all the fields generated by the numerical model. They also gave us an insight to the local balances between the terms. We notice that extra mass and vorticity is entering the basin via rings and this is what affects the vorticity balance. Vigorous motion is felt in the basin due to the ring shedding and its major impact is on the stretching term. This vortex stretching has an impact on the thermocline motions which will adjust thermohaline circulations that are of most interest.

From the momentum balances we had obtained an important result from comparing two scenarios sought from the real world, where either the ACC or the Agulhas leakage provides a northern flow out the basin. It remains to be shows by measurement which momentum balance is actually occurring. However, we find the combined vorticity and momentum balances from the Agulhas leakage gives us a good inclination that this is the likely real world situation occurring and informs that it has a major influence on the Thermohaline Circulation.

We now understand that the large contributions of stretching and friction within the South Atlantic are due to Agulhas rings shed in the basin. Each ring shed may have a different effect to which we are unable to comment. The shedding of rings introduces saltier, warmer water into the South Atlantic. The Indian Ocean has approximately $5°C$ warmer water and is about $0.3 - 0.4\,psu$ greater than the South Atlantic (Gordon, 1985). The impacts of the spawning of rings in the South Atlantic can play an important role on the Overturning Circulation present in the Atlantic Ocean which is based on the heat input and freshwater fluxes.

The impact of the Agulhas leakage and its ring shedding in the Atlantic Ocean has been linked to historic events. We believe the Agulhas leakage may explain past events but also is an important area of study especially for future climate projections. The Younger Dryas period that happened around 12,000 years ago was accompanied by a shutdown of the Overturning Circulation (Broecker, 1991). Introducing freshwater into the oceans, especially the Atlantic is a likely reason to why the conveyor has and could shutdown.

The rings provide salt and heat into the Atlantic Ocean that could be crucial to maintaining an Overturning Circulation without it shutting down, something we

should be aware of for the future. From Climate Change studies, we expect that with a shutdown of the conveyor we could undergo an abrupt climate change similar to the Younger Dryas period which could affect climate conditions. The consequences could mean the arrival of cold and harsh weather particularly to Western Europe and Northern America.

In this study, the Agulhas leakage has only been assessed on a two-layer reduced gravity model to give us an understanding of the momentum and vorticity balances in the South Atlantic Ocean. Further study remains essential to our understanding of the Atlantic and Indian Oceans with the involvement of the Agulhas leakage.

Improved numerical models that have a higher resolution; incorporate a more detailed structure of the African island and possibly include information on the bottom topography of the Indian Ocean near Africa could provide a more accurate picture of the rings being shed into the basin and their possible impacts. There are also other aspects that could be considered to improve our understanding of what is occurring. For instance we could include additional information about seasonal variability and extending our two-layer model to a multi-layer model. Including these aspects mentioned can help provide a detailed illustration of how exactly the Agulhas rings move into the ocean basin and assess any further impacts.

# 9 Summary

The Agulhas area south of Africa is where the Indian Ocean meets with the South Atlantic Ocean. The Agulhas Current flows into the South Atlantic then retroflects back into the Indian Ocean carrying most of its mass transport back with it. Where this current enters and its retroflection takes place is known as the Agulhas leakage. We are concerned with the influence this has on the Overturning Circulation. Throughout, we have used a two-layer reduced gravity model and integrated the given momentum and vorticity equations on the South Atlantic Ocean. Each variable used has its own approximated order of magnitude for a large-scale ocean circulation in the South Atlantic.

We began with a closed basin, having no mass transport entering or leaving. The momentum balances ultimately provided us with information about the depth of the active layer. We find that the depth is approximately equal at the eastern and western boundaries of the basin but also, it is deeper at the northern boundary in comparison to the southern boundary. Furthermore, we found that the momentum equation in the meridional direction told us that the gyre is governed by a balance dominated by the pressure gradient and Coriolis terms. The use of a numerical model confirmed these depth related results.

The next step was to apply the integrated vorticity equation on the closed basin; found by taking the curl of the momentum equations. Vorticity is used to give us a measure the spin within the basin. We learned that the diffusivity parameter had to be an order of magnitude larger for this equation to balance correctly. A larger diffusivity takes into account eddy diffusion associated with turbulent fluids. It also suggests that there is a time dependence. This was considered in our numerical model; it allowed time-averaging of the vorticity terms after the model reaches a statistical equilibrium.

Furthermore, in terms of the diffusivity we had to recheck the momentum balance. The inclusion of a larger diffusivity parameter within the friction term still gave us the same momentum balance between the Coriolis and pressure term. Most importantly, we discovered that this coefficient can vary in the South Atlantic Ocean. We held the same diffusivity parameter throughout for the analytical studies of the momentum balances. However, the time-averaged terms in the numerical model had a larger effective value for the eddy diffusivity.

Systematically, different configurations were then set up aiming to build up to the real world scenario. This meant that the basin had to be adjusted to having open boundaries. The real world configuration that we were to achieve includes the Agulhas leakage and Antarctic Circumpolar Current (ACC) flowing into the South

Atlantic. From looking at these currents flowing in, the aim was to find which one of the two currents could provide a momentum balance if only one of them were to provide the outflow we have at the northern boundary of the basin.

In the scenarios building up to this, we first adjusted the basin to allow mass transport to enter the south and then exit out at the north of the basin, both adjacent to the western boundary. This scenario gave us a momentum balance proving geostrophic balance, where the Coriolis force was balanced by an opposing pressure gradient force. We then amended this scenario to removing the northern outflow and adding an outflow at the opposite end of the southern boundary. We then found there was only a geostrophic balance in the meridional direction, the zonal direction gave us a similar finding to the closed basin scenario.

Upon combination of the two scenarios above, the resulting scenario was built where the ACC entered and left the basin. However, adjustments were made to the amount of mass transport entering and leaving in order to represent this flow. Continuing with the application of the momentum balances again proved a geostrophic relationship, this time in both directions.

Following the scenario of the ACC, we moved on to an Agulhas leakage setup. This initial Agulhas leakage setup was where all mass transport entered the basin on the eastern boundary and left on the same boundary. The idea was that transport entering, all retroflects back into the Indian Ocean. This configuration proved once again a geostrophic relationship but we noticed the advection term in the zonal direction was larger than the previous cases. We recognised that we should be aware of errors in estimates here, which could make terms larger or smaller than expected. However, we suggested here that the pressure term should be similar to the Coriolis term as this is what we experienced in the scenarios prior to this.

Our next task was to adjust the Agulhas leakage situation so it could account for mass transport leaving the basin at the northern boundary. We understand that the shedding of Agulhas rings takes place within the South Atlantic and it was of interest to look at the momentum balances for the existence of additional transport coming from the Agulhas leakage and leaving at the other end of the basin.

We found that in the zonal momentum equation, an advection term was present in the balance as well as the expected Coriolis and pressure gradient terms. This outcome portrayed an ageostrophic nature of the fluid flow within the basin. It was suggested here that the pressure gradient term may have been small and therefore, left with a balance involving the advection and Coriolis terms. The meridional balance had also shown that we have local geostrophy present but the large-scale integrated balance was different. We saw this here, as although we have a net westward flow, the eastward flow being further south gives rise to a stronger

Coriolis force. This meant that the momentum balance was different to the previous scenarios and we began to find more interesting results.

Having looked at the different scenarios of mass transport in and out of the basin, we were in the position to look at the full problem. The problem put forward was that either the ACC or the Agulhas leakage provided the outflow at the northern boundary of the basin.

The main outcome of the problem was related to the depths at the east and west boundaries of the basin. The ACC problem gave us an insight to the western boundary being deeper than the eastern boundary and the opposite was found for the Agulhas leakage.

The previous scenarios had shown balances that were related to geostrophy whilst some were not; these had an involvement from an advection term. The two scenarios here both had a momentum balance in the zonal direction that involved an advection term as well as a Coriolis term. In order to balance the equation fully, the pressure term was derived from these two terms. Positive for the Agulhas leakage and negative for the ACC; this is how we were able to describe the depth at the two boundaries. Both results proved interesting and without further study of the basin itself, we remain unable to comment on what situation exists in the South Atlantic.

In light of this, we turned to vorticity to obtain further information about the Agulhas leakage and what its impacts are on the South Atlantic. We returned to the numerical model to provide us with the a simulation of the real world Agulhas leakage and an idea of the typical vorticity balances.

The numerical model was able to calculate time-averaged terms in the vorticity equation. The closed basin model gave rise to a balance between the wind-stress and friction terms. We already seen in the analytically integrated vorticity equation that this was the case. However, we found an important result from the open basin. We noticed that the vorticity balance was dominated by friction, wind-stress and stretching terms. This vorticity balance gives us an idea of the influence the Agulhas leakage has on the South Atlantic Ocean and also the Overturning Circulation.

The vorticity fields were able to show the local balances of the open island case. However, the balance seen was the stretching and Beta term balancing with the friction term. We know from the integrated terms that the balance included wind-stress; the fields did not show this because the term was small and positive but once integrated over the whole basin it became large and dominant. Numerical outputs of the open island show vorticity being input into the basin from the Agulhas leakage and we notice that these have an influence on the large-scale balances.

# 10 Conclusion

The influence the Agulhas leakage has on the South Atlantic is determined by the salt and heat input via these Agulhas rings that spawn in this basin. The momentum balances suggest that these rings are the reason for mass transport leaving north of this basin, given a certain amount of uncertainty not being too large. The momentum balance show signs of local geostrophy but also a contribution from zonal advection into the basin, from which we can infer the depth at the eastern boundary is deeper than the western boundary. Further study is encouraged to support the claim that the Agulhas leakage provides a northern outflow and is also to be done with regards to the active layer depth.

The numerical model shows Agulhas rings moving into the basin and that they have a significant impact on the vorticity balance. We understand from this that these rings must have an impact on the Overturning Circulation. The idea is focused on the heat and salt input into the basin by the rings which transport mass from the Indian Ocean. In the time-integrated vorticity balance, we found the appearance of a stretching term which suggests a large impact on thermocline motions in turn having an impact on the Thermohaline Circulation.

We understand the concept behind the Overturning Circulation; based on heat and salinity fluxes around the worlds oceans. We imagine the situation where the Agulhas rings do not spawn in the Atlantic Ocean. The salinity and heat input would be lowered. We have mentioned a shutdown of the oceans conveyorbelt can be caused by an increased amount of freshwater fluxes into the oceans. A lack of salinity is equally interpreted as an increased amount of freshwater. We know the momentum and vorticity balances are conserved by the Agulhas leakage into the South Atlantic Ocean. It must play an important role in maintaining the ocean's Overturning Circulation.

# 11 References


Broecker, W. S. (1991). The great ocean conveyor. *Oceanography*. **4**, 79-89.

De Ruijter, W. P. M., A. Biastoch, S. S. Drijfhout, J. R. E. Lutjeharms, R. P. Matano, T. Pichevin, P. J. Van Leeuwen and W. Weijer. (1999). Indian-Atlantic intero-cean exchange: Dynamics, estimation and impact *J. Geophys. Res.* **104**, 20885-20910.

De Ruijter, W. P. M., P. J. van Leeuwen and J. R. E. Lutjeharms. (1999). Generation and evolution of Natal Pulses: solitary meanders in the Agulhas Current. *J. Phys. Oceanogr*. **29**, 3043-3055.

Gates, W. L. (1972). On the reynolds stress and lateral eddy viscosity due to transient oceanic Rossby waves. *Pure and Applied Geophysics*. **96**, 217-227.

Gordon, A. L. (1985). Indian-Atlantic transfer of thermocline water at the Agulhas Retroflection. *Science*. **227**, 1030-1033.

IPCC. (2001). *Climate Change 2001: The Scientific Basis. Contribution of Working Group I to the Third Assessment Report of the Intergovernmental Panel on Climate Change*. Cambridge. Cambridge University Press.

Leeuwen, P. J., and W. P. M. de Ruijter. (2009). On the steadiness of separating meandering currents. *J. Phys. Oceanogr*. **39**, 437-448.

Leeuwen, P. J., W. P. M. de Ruijter, and J. R. E. Lutjeharms. (2000). Natal pulses and the formation of Agulhas Rings. *J. Geophys. Res.* **105**, 6425-6436.

Lutjeharms, J.R.E and R.C. van Ballegooyen. (1988). The Retroflection of the Agulhas Current. *J. Phys. Oceanogr.*, **18**, 1570-1583.

Nof, D. and T. Pichevin. (1996). The retroflection paradox. *J. Phys. Oceanogr*. **26**, 2344-2358.

Nof, D. (2005) The momentum imbalance paradox revisited. *J. Phys. Oceanogr*. **35**, 1928-1939.

Peterson, R. G., L. Stramma. (1991). Upper-level Circulation in the South Atlantic Ocean. *Prog. Oceanogr.* **26**, 1-73.

Pichevin, T., D. Nof and J. Lutjeharms. (1999). Why are there Agulhas rings?. *J. Phys. Oceanogr*. **29**, 693-707.

Pinet, P. R. (2009). *Invitation to Oceanography*. 5th ed. London, United Kingdom: Jones and Bartlett.

Rintoul, S., Hughes, C., Olbers, D. (2001). The Antarctic Circumpolar Current System. In: *Ocean Circulation and Climate*. (G. Siedler, J. Church and J. Gould, eds.) London, United Kingdom: Academic Press. 271-302.

Vallis G. K. (2006). *Atmospheric and Oceanic Fluid Dynamics: Fundamental and Large-Scale Circulation*. New York, United States of America: Cambridge University Press.

Whitworth, T., (1983). Monitoring the Transport of the Antarctic Circumpolar Current at Drake Passage. *J. Phys. Oceanogr.* **13**, 2045-2057.

Whitworth, T., R. G. Peterson. (1985). Volume Transport of the Antarctic Circumpolar Current from Bottom Pressure Measurements. *J. Phys. Oceanogr.* **15**, 810-816.